

Discovery of Small Molecule Cyclic GMP-AMP Synthase Inhibitors

Rosaura Padilla-Salinas, Lijun Sun, Rachel Anderson, Xikang Yang, Shuting Zhang, Zhijian J. Chen, and Hang Hubert Yin

J. Org. Chem., **Just Accepted Manuscript** • DOI: 10.1021/acs.joc.9b02666 • Publication Date (Web): 12 Dec 2019

Downloaded from pubs.acs.org on December 12, 2019

Just Accepted

“Just Accepted” manuscripts have been peer-reviewed and accepted for publication. They are posted online prior to technical editing, formatting for publication and author proofing. The American Chemical Society provides “Just Accepted” as a service to the research community to expedite the dissemination of scientific material as soon as possible after acceptance. “Just Accepted” manuscripts appear in full in PDF format accompanied by an HTML abstract. “Just Accepted” manuscripts have been fully peer reviewed, but should not be considered the official version of record. They are citable by the Digital Object Identifier (DOI®). “Just Accepted” is an optional service offered to authors. Therefore, the “Just Accepted” Web site may not include all articles that will be published in the journal. After a manuscript is technically edited and formatted, it will be removed from the “Just Accepted” Web site and published as an ASAP article. Note that technical editing may introduce minor changes to the manuscript text and/or graphics which could affect content, and all legal disclaimers and ethical guidelines that apply to the journal pertain. ACS cannot be held responsible for errors or consequences arising from the use of information contained in these “Just Accepted” manuscripts.

Discovery of Small Molecule Cyclic GMP-AMP Synthase Inhibitors

Rosaura Padilla-Salinas¹, Lijun Sun², Rachel Anderson¹, Xikang Yang³, Shuting Zhang³, Zhijian J. Chen^{2, *} and Hang H. Yin^{1,3, 4, *}

¹Department of Chemistry and Biochemistry and Biofrontiers Institute, University of Colorado Boulder, Boulder, CO 80309-USA

²Department of Molecular Biology, University of Texas Southwestern Medical Center, Dallas, TX, 75390-9148, US; ^bHoward Hughes Medical Institute, University of Texas Southwestern Medical Center, Dallas, TX 75390-9148; ^cDepartment of Immunology, University of Texas Southwestern Medical Center, Dallas, TX, 75390-9148; ^dAnimal Resource Center, University of Texas Southwestern Medical Center, Dallas, TX, 75390-9 148

³School of Pharmaceutical Sciences, Tsinghua-Peking University Center of Life Science, Tsinghua University, Beijing 100082, China

⁴Lead contact

*Correspondence: yin_hang@tsinghua.edu.cn (H. H. Y.) and zhijian.chen@utsouthwestern.edu (Z. J. C.)

Abstract

Cyclic GMP-AMP (cGAS), a cytosolic DNA sensor, plays an important role in the type-I-interferon response. DNA from either invading microbes or self-origin triggers the enzymatic activity of cGAS. Aberrant activation of cGAS is associated with various autoimmune disorders. Only one selective probe exists for inhibiting cGAS in cells while others are limited by their poor cellular activity or specificity, which underscores the urgency for discovering new cGAS inhibitors. Here, we describe the development of new small molecule human cGAS (hcGAS) inhibitors (80 compounds synthesized) with high binding affinity in vitro and cellular activity. Our studies show CU-32 and CU-76, selectively inhibit the DNA pathway in human cells but had no effect on RIG-I-MAVS or Toll-like Receptor pathways. CU-32 and CU-76 represent a new class of hcGAS inhibitors with activity in cells and provide a new chemical scaffold for designing probes to study cGAS function and development of autoimmune therapeutics.

cGAS-STING signaling, inflammation, type-I interferon, autoimmune, cyclic GMP-AMP synthase, inhibitor

INTRODUCTION

1
2 In the cytosol, microbial RNA with specific features can be recognized by Retinoic acid-Inducible Gene I (RIG-I) or Melanoma Differentiation-
3 Associated protein 5 (Mda5), which activate Mitochondrial Anti-Viral Signaling protein (MAVS). As an adaptor protein, MAVS recruits and acti-
4 vates Tank-Binding Kinase 1 (TBK1) complex and Inhibitor of κ B Kinase (IKK) complex. On the other hand, cytosolic DNA is detected by the
5 cyclic GMP-AMP synthase (cGAS), a primary DNA sensor that belongs to the nucleotidyltransferase enzyme family.^{1,2,3} Upon dsDNA recognition,
6 cGAS catalyzes the formation of cyclic dinucleotide, cyclic GMP-AMP (cGAMP or c[G(2',5')pA(3',5')p]). As a second messenger, cGAMP binds
7 to the adaptor protein stimulator of interferon genes (STING) and triggers its cellular trafficking and activation of TBK1 and IKK complexes. In both
8 RIG-I/MAVS and cGAS/STING pathways, TBK1 and IKK activate the transcription factors Interferon regulatory factor 3 (IRF3) and Nuclear Factor
9 kappa-light-chain-enhancer of activated B cells (NF- κ B), which are essential for induction of type I interferons and other inflammatory cytokines.
10
11
12
13
14
15

16 Unlike many other nucleic acid sensors, cGAS does not distinguish self- from non-self-DNA, therefore aberrant accumulation of self-DNA in the
17 cytoplasm can induce unwanted immune response.² Normal cells deploy multiple DNases including Trex1 to keep cytoplasm clear of DNA. In the
18 absence of functional Trex1, endogenous DNA can activate cGAS-STING pathway.⁴ Recent studies in mice and humans have shown that dysregu-
19 lation of the cGAS-STING pathway leads to uncontrolled chronic inflammation and autoimmunity.^{3,4,5} For example, multiple mutations in Trex1
20 gene are associated with Aicardi-Gouti es syndrome (AGS). Mice deficient in the TREX1-gene develop lupus-like syndrome and die prematurely
21 from multi-organ inflammation.^{6,7} Gain-of-function mutations within STING in human patients are linked to early onset STING-associated vascu-
22 lopathy, an autoinflammatory disease.⁸ Lastly, cGAS-STING signaling has also been shown to promote cancer growth and metastasis through mod-
23 ulation of the tumor microenvironment.⁹
24
25
26
27
28
29

30 Crystal structures of the cGAS dimer bound to dsDNA have provided valuable insight into the activation mechanism of cGAS. However, in order
31 to interrogate the physiological function of cGAS in a cellular context, chemical tools that selectively modulate cGAS enzymatic activity would be
32 of great value. The central role of cGAS-STING pathway in inflammation, autoimmunity, cancer, and tumor progression has spurred intensive
33 investigations toward the identification and characterization of small molecule inhibitors for cGAS, including **RU.521**, **PF-06928215**, suramin, and
34 **X6**. Although these modulators all have demonstrated antagonistic effects on cGAS, the inhibitors are also associated with drawbacks that may limit
35 their utility as cellular chemical tools. The compound **RU.521** is a potent small molecule inhibitor of murine cGAS (mcGAS), and **PF-06928215**
36 only inhibits human cGAS (hcGAS) but lacks cellular activity. Suramin, an approved drug, and amino acridine, **X6** were also identified as viable
37 cGAS inhibitors.¹⁰⁻¹¹ Unlike **RU.521** and **PF-06928215**, suramin and **X6** inhibit hcGAS and mcGAS, respectively, through the displacement of DNA
38 from cGAS.^{12,13} Although suramin is active in human cells, the inhibitor suffers from off-target effects through inhibition of the Toll-like receptor
39 (TLR) 3 dsRNA sensing pathway. This year, a new post translational modification for regulation of cGAS was discovered and led to reprofiling of
40 aspirin as a potential cGAS inhibitor in humans (*vide infra*).¹⁴ Indeed, only few small molecule cGAS inhibitors exist, highlighting the urgent need
41 to discover new chemical scaffolds that can selectively inhibit hcGAS in cells.
42
43
44
45
46
47
48
49

50 Inspired by the crystal structure studies describing the activation loop and the mutagenesis experiments demonstrating the essential role of the
51 two DNA binding surfaces and the protein-protein interface (PPI) of cGAS for IRF3 activation and IFN- β induction, we decided to take an innovative
52 rational approach to target the PPI of hcGAS as a means to inhibit its enzymatic activity.¹⁵ In this manuscript, we describe the successful identification
53
54
55

of a new chemical scaffold and the development of a new small molecule inhibitor targeting PPI of hcGAS with in vitro and cellular activity in human monocyte THP-1 cells.

RESULTS and DISCUSSION

Strategy for discovering a small molecule hcGAS inhibitor. Crystallographic studies of the 2:2 mcGAS complex with DNA revealed several key residues involved in the PPI and cGAS-DNA interaction for mcGAS and are shown in Figure 1A.¹⁵ Notably, point mutations studies demonstrated that Lys335 (Lys347 in human cGAS) is essential and involved in mediating the formation of the cGAS dimer. cGAS activity was also abolished in cGAS mutants with point mutations of both Lys335 and Lys382 (Lys 394 in humans), demonstrating their critical role for cGAS function. Furthermore, a group demonstrated hcGAS can be inhibited by aspirin mediated acetylation of either Lys384, Lys394, or Lys494 in patient cells.¹⁴ These results highlighted a potential druggable pocket and motivated us to develop a new approach directly targeting the PPI of cGAS using a virtual screen with a grid-ligand binding box that incorporated Lys335 and Lys382, See Figure 1B. Importantly, these recent findings also provide additional evidence for targeting residues, in particular Lys384, Lys394, or Lys494, involved in DNA binding to cGAS.

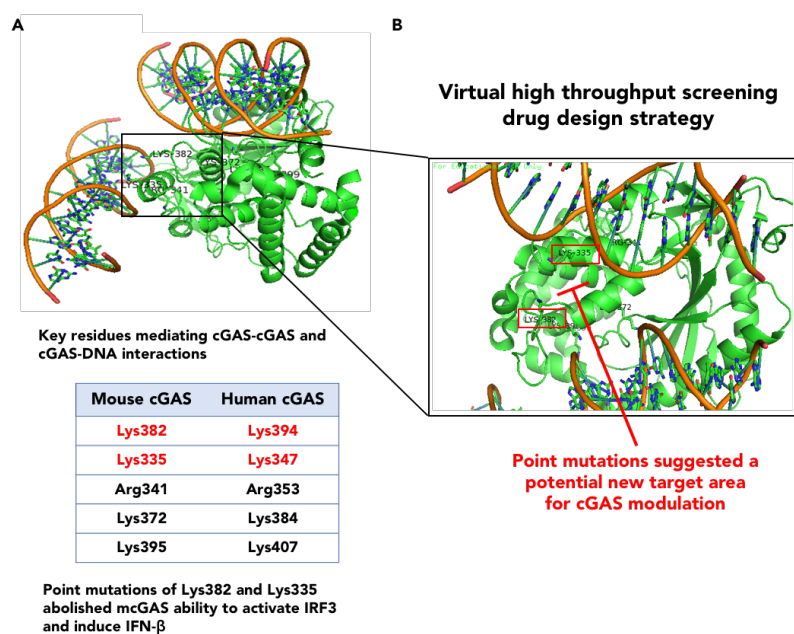


Figure 1. Residues mediating important cGAS-cGAS and cGAS-DNA interactions and the design of an unprecedented strategy for inhibiting hcGAS.

(A) Schematic of mcGAS and dsDNA interaction surfaces. The residues highlighted in red are involved in the dimer interface of cGAS and mediate cGAS-DNA interactions. (B) Close-up view of the grid generated on the PPI of mcGAS. For the virtual high throughput screen of the Maybridge and Enamine drug databases, the grid box was generated to target the PPI of mcGAS with incorporation of important residues mediating the PPI interactions.

Virtual screen results and discovery of a small molecule hcGAS inhibitor. Using the strategy described above, we performed a high throughput virtual screen (HTVS) of drug-like libraries against the cGAS/dsDNA complex to identify novel small molecule hcGAS inhibitor. An in-silico screen of the Maybridge (53,000 compounds) and Enamine (1.7 million compounds) Hit finder libraries using the Glide 5.6 program was conducted using reported co-crystal structures of recombinant mcGAS, since hcGAS-DNA complex was unknown until recently.¹⁶ Based on the findings described

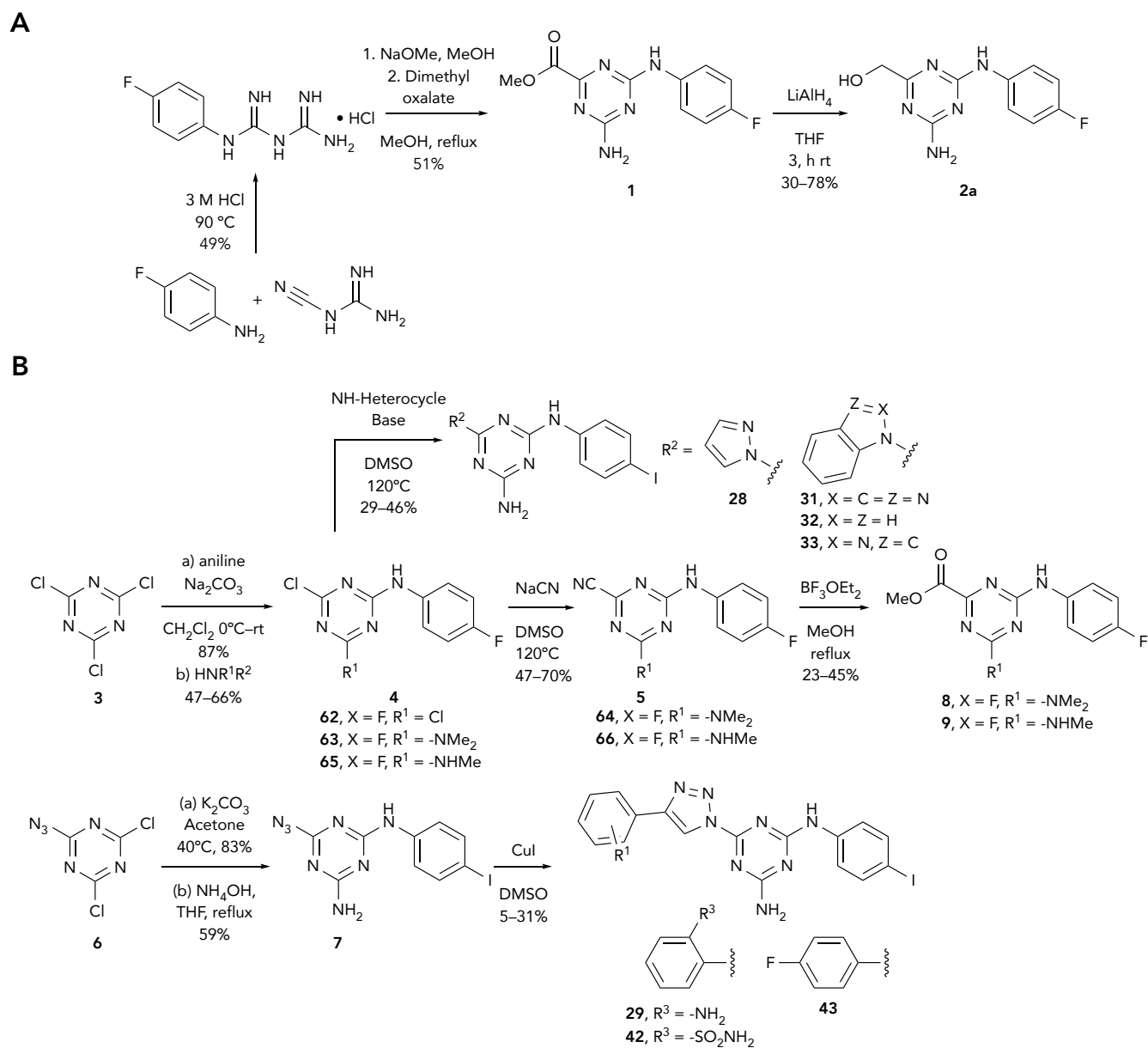
1 above, we generated the grid on the PPI with incorporation of the residues involved in the dsDNA binding site (crystal structure PDB ID: 4O6A),
2 see Figure 1B.^{17,18}
3

4 We identified ten small molecules hits from the in-silico screen, see Supplemental Figure S1 and Table S1. The selection of the candidate mole-
5 cules was based on four criteria: (1) predicted binding energy and spatial complementarity; (2) reasonable chemical structures found in the dsDNA-
6 binding site of cGAS; (3) existence of at least one hydrogen bond between the ligand and one of the dsDNA-recognizing residues on the cGAS
7 surface; (4) drug-like properties analysis. Drug-like properties considered in this study follow Lipinski's rule of five and include properties such as
8 molecular weight, hydrogen bond or, hydrogen bond acceptor, Lipophilicity (log P), and human oral absorption. From the initial hits validated, only
9 one hit inhibited hcGAS, **Z918**, at 100 μ M in the in vitro activity assay, see Supplemental Figure S1.¹⁹ Notably, **Z918** was the only hit with a
10 heterocyclic core similar to **PF-06928215**. Preliminary in vitro data for **Z918** displayed sufficient inhibitory activity against hcGAS to advance
11 potency optimization. Additionally, all efforts have only focused on targeting the catalytic pocket of cGAS or the dsDNA/cGAS protein-nucleic acid
12 interface through the displacement of dsDNA. In contrast, our innovative approach targets the PPI of hcGAS and provides an opportunity to possibly
13 overcome the selectivity shortcomings of current cGAS inhibitors via the discovery of a new scaffold and a druggable binding pocket.
14
15
16
17
18
19
20

21 **Synthesis overview of the designed hcGAS inhibitor 1 and related molecules.** To rapidly discover a novel potent hcGAS inhibitor, we used
22 synthetic routes amenable to high throughput synthesis and designed versatile intermediates that could be diversified to different classes of target
23 compounds. Methyl 4-amino-6-[(4-fluorophenyl)amino]-1,3,5-triazine-2-carboxylate (**1**) was synthesized using a reported one-pot cyclisation con-
24 densation reaction of the N'-(azaniumylmethanimidoyl)-N-(4-fluorophenyl)guanidine chloride with dimethyl oxalate See Figure 1A.¹⁸ This strategy
25 was robust for the synthesis of several 4-amino-6-(arylamino)-1,3,5-triazine-2-carboxylate derivatives with various substitutions of different size and
26 electron withdrawing (EWG)/donating (EDG) capabilities on the N2-phenyl ring. Reduction of compound **1** with lithium aluminum hydride (LiAlH₄)
27 afforded **2a** in 30–78% yield, See Figure 1A. See Supplemental Experimental Procedures and Scheme S1–S8 for the synthesis of **7–15** compounds.
28 Rapid diversification of the 6-position of the 1,3,5-triazine core was achieved using temperature controlled nucleophilic aromatic substitution (S_NAr)
29 of the -Cl atoms on commercially available cyanuric chloride, see Scheme 1B. This synthetic route was appealing because it was a scalable route
30 that provided access to multiple symmetrical and unsymmetrical substituted analogs in 3 steps. Based on the SAR results described below we only
31 pursued unsymmetrical 2,4,6-substituted triazine analogs with a focus on analogs bearing a 2° aniline and -NH₂ group at the 2- and 4-positions
32 respectively. Intermediates **4** and **7** were synthesized from commercially available cyanuric chloride (**3**) and 2-azido-4,6-dichloro-1,3,5-triazine (**6**)
33 via S_NAr with varying nucleophiles in moderate yields, see Scheme 1B. These compounds were then further functionalized with different commer-
34 cially available building blocks for the synthesis **27–33** targets, see Supplemental Experimental Procedures and Supplemental Scheme S11–S12.
35 Overall, the modular synthetic approaches allowed us to diversify the core scaffold, culminating in the synthesis of 80 distinct novel analogues and
36 the discovery of two new leads and an alternative scaffold displaying similar activity compared to top inhibitors, see SAR discussion of bioactivity
37
38
39
40
41
42
43
44
45
46
47
48
49
50
51
52
53
54
55
56
57
58
59
60

results below and Supplemental Experimental Procedures, Supplemental Scheme S9–S13 for additional syntheses, and Supplemental Table S3–S5

for additional SAR.



Scheme 1. Synthesis of 1, 2a and related compounds. (A) Schematic representation of the one-step condensation cyclisation reaction for the synthesis of 4-amino-6-(arylamino)-1,3,5-triazine-2-carboxylate derivatives. (B) Schematic representation of select 6-substituted 4-amino-6-(arylamino)-1,3,5-triazine derivatives. (C) Synthetic routes for targets are summarized in the supplemental information (see Supplemental Experimental Procedures and Supplemental Scheme S1–S14.)

Discovery of a small molecule inhibitor targeting hcGAS. Initially thirteen analogs were designed to identify key structural motifs contributing to the active pharmacophore and structure activity relationship (SAR) trends to improve the bioactivity of the putative lead, **Z918**. The ester functionality was identified as a metabolically unstable group as it can be hydrolyzed by an esterase. To test this concept, we first synthesized the primary

alcohol, **2a**, the hydrolysis product of **Z918** and -OMe (**2b**) as the H-bonding control for **2a**. A 20-fold increase in potency compared to **Z918** was observed with **2a** in vitro, Figure 2. We hypothesized the lower in vitro activity of **Z918** could be due to poor binding caused by the steric bulk of the large hydrophilic anthranilic acid motif. The amine (**2c**) and ester (**1**) functional groups at the 6-position were also examined. Compound **1** with the ester functional group was identified as the most active inhibitor, and Figure 2.

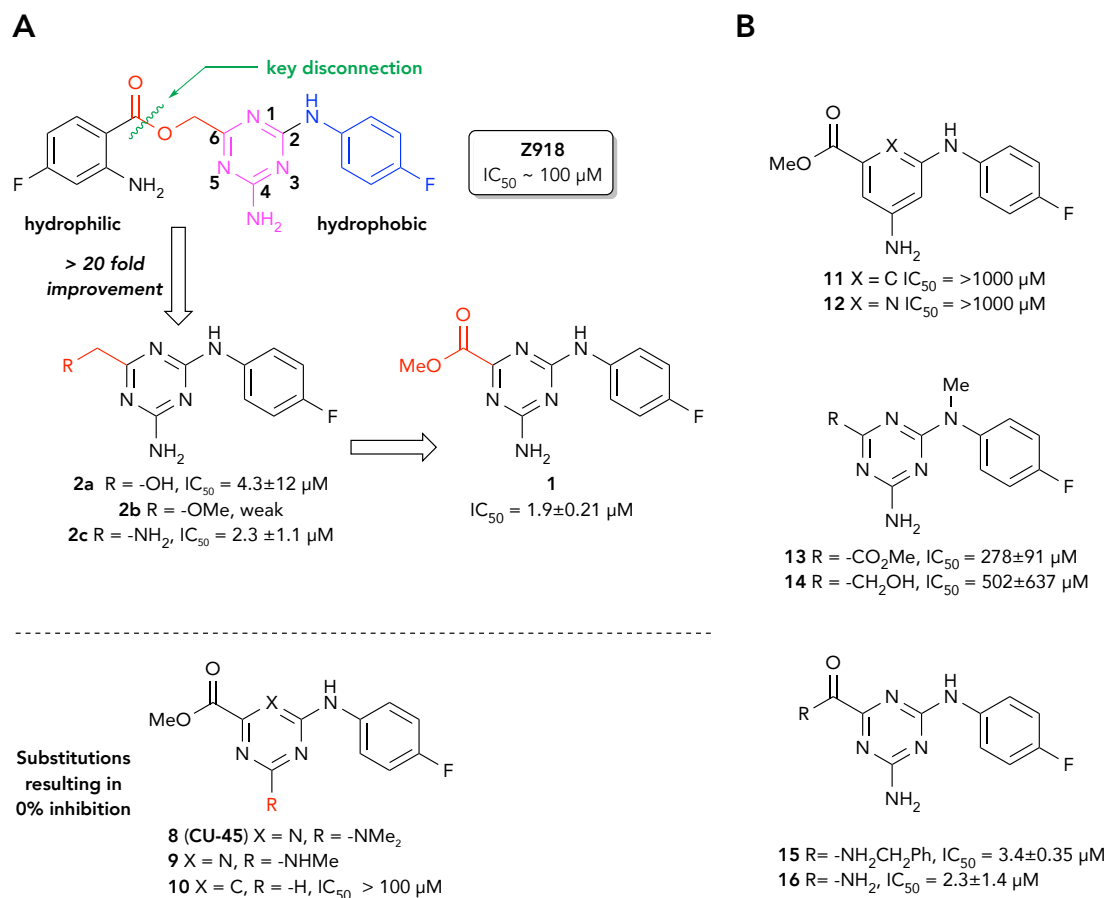


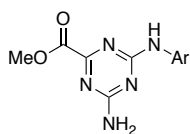
Figure 2. Preliminary SAR studies for hcGAS inhibitors. (A) Targets synthesized to identify key protein binding structural motifs. (B) Structures of additional derivatives designed to probe inhibitor interactions.

We then focused on systematically altering the 4-amino group and the heterocyclic core, see Figure 2A and 2B. Interestingly pyrimidine **10**, lacking the 4-NH₂ group was active at 100 μM, implying a critical role for the 4-NH₂ group. Replacement of the 1,3,5-triazine core with a benzene ring (**11**) abrogated the bioactivity, indicating an electron deficient heterocyclic core is necessary. We ruled out 4-aminopyridine **12** (>1000 μM) and pyrimidine **10** (>100 μM) scaffolds because inhibition was only observed at very high concentrations. Thus, the methylated derivatives of **8** (CU-45) and **9** were prepared to further investigate the impact of the amine substitution. Methylation of the 4-NH₂ group resulted in complete loss of activity. These results implied a functional group with a combination of H-bond donating/accepting capabilities at the 4-position is critical to the bioactivity. We rationalized the loss in activity for **8** and **9** could be due to steric effects. Because the 4-NH₂ group was key to the activity, we prepared an additional derivative with a tertiary aniline at two position, compound (**13**), to systematically establish the importance of the presence of the -NH bond. We also observed a significant decrease in inhibitory activity for compound **13** (IC₅₀ = 278 ± 91 μM, see Figure 2B.). These results helped us

identify an additional position where a combination of H-bond donating/accepting capabilities is critical to the bioactivity. Compound **1** was advanced to chemical optimization due to its high activity and ease of synthesis.

Improving CU-1 potency through SAR. We first prepared several 4-amino-6-(arylamino)-1,3,5-triazine-2-carboxylate derivatives with various substitutions of different size and electron withdrawing (EWG)/donating (EDG) capabilities on the N2-phenyl ring. See Scheme 1 for synthesis. Keeping the 2-phenylamino ring, we replaced the -F with -H (**17**) and -CF₃ (**18**) and this decreased inhibitory activity indicating electronics is the dominating factor rather than size. Therefore, we examined other halogens and introduced EWG at the *para*-position. Substitution of -F with -I led to 3 orders of magnitude increase in potency with compound (**19**) (IC₅₀ = 0.45 μM), Table 1. By contrast, substitution at the *meta*- (**20**) and *ortho*- positions (**21**) with -I decreased potency demonstrating the *para*- position is optimal. EWG (-NO₂, -CN, and -CF₃) and electron donating groups (-OH and -OMe) with H-bond donating/accepting capabilities were less active, Supplemental Table S3. Replacement of the 2-phenylamino ring with other heteroaromatic groups such quinoline, did not improve the activity. Unlike fluorine, iodine can engage in halogen bonding, an electrostatically driven interaction.¹⁸ To further explore this, we examined the ethynyl group, as previous investigators have shown it can be used as an iodine bioisostere.²¹ The ethynyl group is a nonclassical bioisostere that has a polarized -CH moiety, and it is a weak hydrogen bond donor.²⁴ For our inhibitors, replacement of -I with the ethynyl moiety (**24**) did not improve the potency, which explained that halogen bonding may not be the dominating factor.¹⁸

Table 1. SAR Analysis for in vitro inhibition of cGAS, Related to Supplemental Table S3.



Compound	Ar	IC ₅₀ (μM)	Compound	Ar	IC ₅₀ (μM) ^b
17	C ₆ H ₅	5.9 ± 1.20	22	4-OH-C ₆ H ₄	8.7 ± 0.69
18	4-CF ₃ -C ₆ H ₄	14.9 ± 1.40	23	4-OMe-C ₆ H ₄	4.5 ± 0.33
19 (CU-32)	4-I-C ₆ H ₄	0.45 ± 0.04	24		1.4 ± 0.03
20	3-I-C ₆ H ₄	3.9 ± 0.16	25		1.5 ± 0.07
21	2-I-C ₆ H ₄	13.1 ± 1.00	26 (CU-76)		0.24 ± 0.01

Ar defined as aryl group. IC₅₀ defined as half maximal inhibitory concentration.

^a In vitro IC₅₀ derived from dose-response curve for the measurement of ATP consumption

from cGAS-mediated 2',3'-cGAMP synthesis. ^b See Supplemental Figure S7 for curves used to generate the reported IC₅₀ values.

To improve the cellular activity of **CU-32**, we modified the 6-position of the 1,3,5-triazine core and the 3- and 5- positions of the NH-phenylamino motif. Replacement of the ester group with heterocycles, such as 1,3,4-oxiazazole (**27**), N- pyrazole (**28**), and aryl-1,2,3-triazoles (**29** and **30**) only showed modest inhibitory activity while benzimidazole (**31**) and indole (**32**) were inactive, see Figure 3 and Supplemental Table S4 for chemical

structures. Finally, 3,4,5-trisubstituted and 3,5-disubstituted phenylamino rings were examined to thoroughly explore additional substitutions on the NH-phenylamino motif. We introduced two F- atoms at the 3- and 5-positions of the NH-phenylamino motif and a ~3-fold increase of inhibitory potency with compound **CU-76 (25)** was achieved showing a low micromolar IC_{50} ($0.24 \pm 0.01 \mu\text{M}$) value. Derivatives with 3,5-disubstitution only showed modest activity suggesting tri-substitution with the I- atom is favorable, see Supplemental Table S5. 2,4,6-trisubstituted analogs were not examined because *ortho*- substituents decreased potency (**20**). Improving the inhibitory activity to the nanomolar range is desirable and would be beneficial for low dosing in the long-term treatment of chronic inflammation pathologies. We believe the micromolar affinities of the triazole inhibitors (compound **29** and **43**) can be further improved to nanomolar range by focusing SAR efforts on 2-aminopenyl-1H-1,2,3-triazole motif and installing groups that increase solubility.

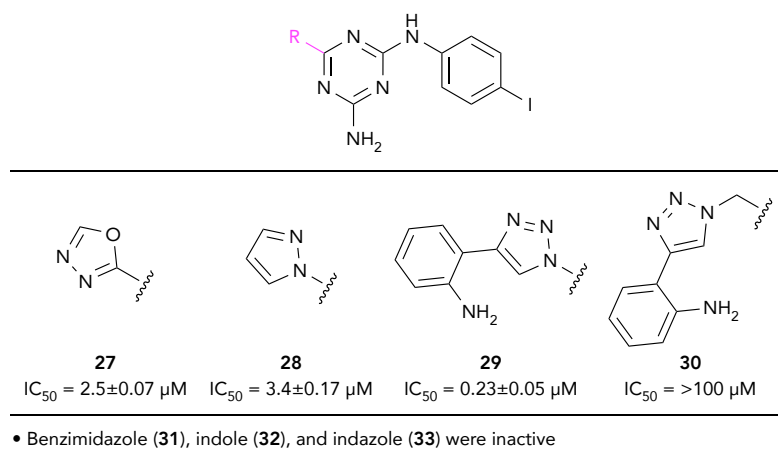


Figure 3. SAR in vitro results for analogs bearing an NH-heterocycles at the six position, Related to Supplemental Table S4. (A) Key targets synthesized to identify protein binding structural motifs. (B) Structure of additional derivatives designed to probe inhibitor interactions. See Supplemental Table S4 for chemical structure of compounds 31–33 and Supplemental Experimental Procedures.

DNA intercalation studies. Selected target compounds from the SAR studies were tested in a high throughput fluorescence polarization (FP) assay for their capacity to intercalate DNA following the protocol developed for **RU.521**.⁹ The five compounds tested showed 0% DNA intercalation compared to mitoxantrone, a known DNA intercalator, see Supplemental Figure S2. The biological investigation for **CU-32** and **CU-76** was prioritized based on stability, potency, and lack of DNA interaction for further testing in cellular assays.

CU-32 analogs selectively inhibit cGAS pathway in human cells. To evaluate cellular activity of selected cGAS inhibitors, we first examined their effects on DNA-induced IRF3 dimerization, which is a hallmark of its activation. Transfection of interferon-stimulatory DNA (ISD), a 45-basepair dsDNA that specifically triggers cGAS-STING pathway, led to strong dimerization of IRF3, which was reduced by both **CU-32** and **CU-76** in a dose-dependent manner (Figure 4A, upper panel). In sharp contrast, **CU-32** and **CU-76** had no effect on Sendai virus-induced IRF3 activation, which is mediated through RIG-I-MAVS pathway, indicating the specificity of these compounds (Figure 4A lower panel). To evaluate their effect on the biological outcome of DNA pathway, we used ELISA to measure IFN- β production from these cells following ISD transfection or Sendai virus infection. **CU-32** and **CU-76** suppressed levels of IFN- β in the media dose-dependently; however, IFN- β levels I response to Sendai virus were

not affected (Figure 4B), confirming the effectiveness and specificity of these compounds. Furthermore, we also confirmed the inhibitory activity of **CU-32** and analogs was not the result of toxicity, as the top inhibitors had no effect on cell viability up to 30 μM , with only partial toxicity at 300 μM (Supplemental Figure S3).

As part of the SAR study, the carboxylic acid derivatives of **CU-1** and **CU-32** were also prepared and determined to have an in vitro IC_{50} value of $3.8 \pm 1.9 \mu\text{M}$ (**1b**) and $0.59 \pm 0.3 \mu\text{M}$ (**19b**), see Figure 4A. for chemical structures. The in vitro inhibitory activity of two amides were determined for compounds **15** at $3.4 \pm 0.35 \mu\text{M}$ and **16** at $\text{IC}_{50} = 2.3 \pm 1.4 \mu\text{M}$, see Figure 2B. for chemical structures. Utilizing a prodrug strategy to optimize effectiveness and “drug like” properties, such as permeability and target selectivity, is a possibility based on the in vitro activities for the carboxylic acid derivatives of **1b** and **19b**.²⁴ However, **1b** did not display antagonistic activity toward the cGAS-STING pathway IRF dimerization assay (See Supplemental Figure S4). Thus, we cannot effectively conclude the active drug is the carboxylic acid of the corresponding methyl ester inhibitor (**1**) since two amide derivatives also inhibited hcGAS in vitro and lacked cellular activity. We speculate the carboxylic acid (**1b**) and amides (**15** and **16**) lack cellular activity due to poor permeability caused by the 4- NH_2 and 2-COOH functional groups.

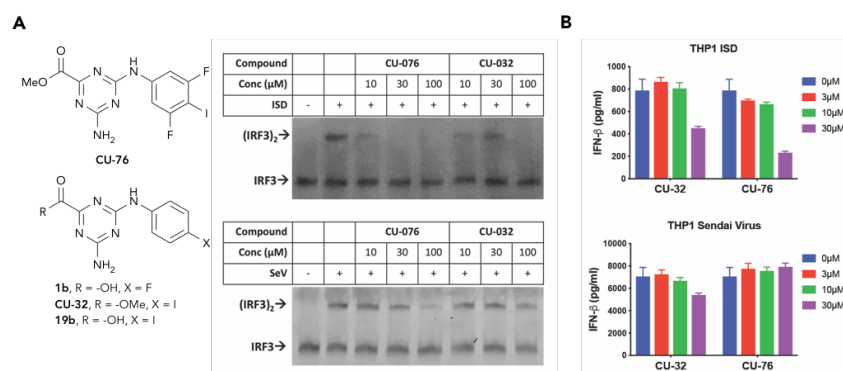


Figure 4. **CU-76** and **CU-32** selectively inhibit the cytosolic DNA sensing, but not the RNA sensing pathway. (A) The interferon regulatory factor 3 (IRF3) dimerization assay with THP-1 cells was used for evaluating cellular inhibitory activity of **CU-76** and **CU-32**. Inhibition of IRF3 activation induced by ISD (upper panel) and Sendai virus (SeV, lower panel) by **CU-32** and **CU-76** in human monocyte THP-1 cells. Readout of cellular dimerization is measured by Western Blotting to detect the interferon regulatory factor 3 dimer (IRF)₂ dimer (0% inhibition = 100% IRF3 dimerization). The (IRF)₂ dimer was not detected at 30 and 100 μM for **CU-76** and at 100 μM for **CU-32** confirming the compounds effectiveness for inhibiting the cGAS-STING pathway. At 10, 30, and 100 μM **CU-76** and **CU-32** did not reduce dimerization of IRF3 induced by the RIG-I-MAVs pathways confirming the specificity of these compounds for the DNA pathway. (B) Effects of **CU-76** and **CU-32** treatment on the production of interferon beta-1alpha (IFN- β) (ELISA measurements) in THP-1 cells stimulated with interferon-stimulatory DNA (ISD) (upper panel) and Sendai virus (Sev). **CU-32** and **CU-76** (10, 30, and 100 μM) suppressed levels of IFN- β in media for ISD stimulated THP-1 cells in a dose dependent manner further supporting the compounds specificity for the DNA pathway. The levels of IFN- β in media were not reduced in THP-1 cells stimulated with Sev showing **CU-32** and **CU-76** (10, 30, and 100 μM) do not display off-target effects for the RNA pathway.

Recent structural and molecular docking studies of the human cGAS-DNA complex defined the species-specificity observed with **RU.521** and **PF-06928215** small molecule inhibitors.¹⁶ We assessed the in vitro and cellular inhibitory activity of **CU-32** and **CU-76** towards mcGAS. Both **CU-**

32 ($IC_{50} = 0.66 \pm 0.10 \mu\text{M}$) and **CU-76** ($IC_{50} = 0.27 \pm 0.06 \mu\text{M}$) inhibited the enzymatic activity of mcGAS in vitro (Figure 5A). In contrast to the effect in THP-1 cells, **CU-32** and **CU-76** were much less effective to suppress DNA-dependent activation of interferon reporter in RAW cells (see Figure 5B and Supplemental Figure S5).

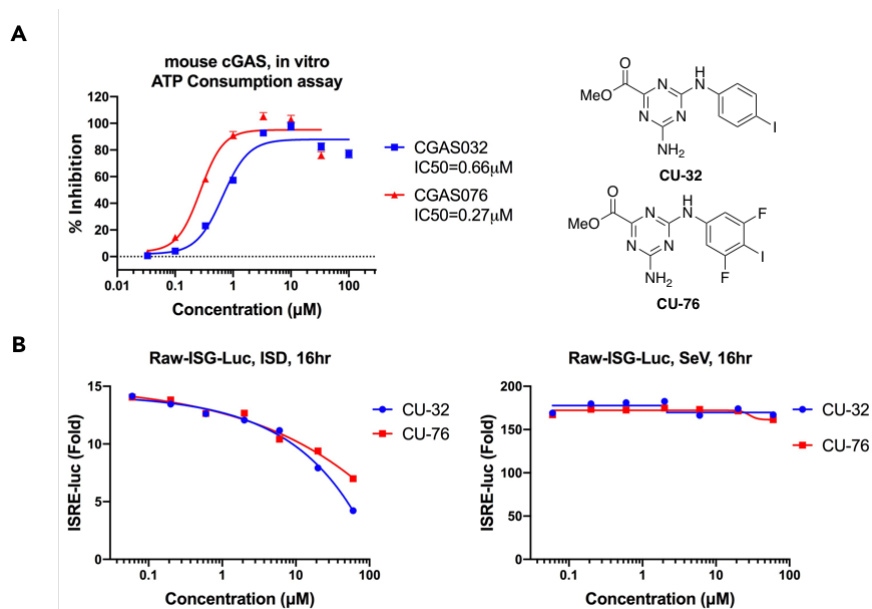


Figure 5. Effect of **CU-32** and **CU-76** on mouse cGAS. (A) In vitro concentration-dependent inhibition of mcGAS enzymatic activity in an ATP consumption assay by **CU-32** and **CU-76**. The IC_{50} value reported represents the mean value. (B) RAW-ISG-luc cells were transfected with interferon-stimulatory DNA (ISD) or infected with Sendai virus (SEV) for 16 h in the presence of serial concentrations of compounds or DMSO, followed by measurement of ISRE reporter expression using luminescence. **CU-32** and **CU-76** were ineffective for suppressing the enzymatic activity of mcGAS in RAW 264.7 cells.

CU-32 does not inhibit Toll-like receptor pathways. To further investigate the selectivity, we tested the effect of **CU-32** on activation of TLR pathways, which are membrane localized pathogen recognition receptors of the innate immune system.²⁶ Various TLRs recognize different viral or bacterial membrane component or nucleic acids. We used human embryonic kidney (HEK) cell lines each ectopically expressing a TLR together with NF- κ B-inducible SEAP (secreted embryonic alkaline phosphatase). Each cell line was stimulated with respective TLR ligands including poly(I:C) for TLR3, LPS for TLR4, R848 and ssRNA²⁷ for TLR7/8, and CpG-ODN for TLR9, in the presence of **CU-32** or DMSO, and activation of TLR signaling was evaluated by measurement of SEAP activity in the media. As shown in Supplemental Figure S6A and Figure S6B., none of the TLR pathways was inhibited by **CU-32** at concentrations up to 50 μM . This compound also had no effect on R848-induced Nitric Oxide (NO) production in Raw cells, see Supplemental Figure S6C. These results further underline the selectivity of **CU-32**.

Molecular docking studies. Because X-ray crystallographic studies did not successfully generate a complex structure, we conducted molecular docking studies to gain insight into the binding mode of **CU-76**. We used mcGAS-DNA (PDB ID: 4O6A) for molecular docking analysis with active (**CU-76**) and inactive cGAS inhibitors (**CU-45**). Based on previously reported crystallographic studies, we utilized relevant key amino acids located on the mcGAS-mcGAS binding interface and DNA binding sites (see Figure 1).³⁰ The molecular docking analysis of **CU-76** against mcGAS-DNA

complex show the inhibitors may bind in the groove aside the Zn loop (see Figure 6A and Supplemental Figure S8). We speculate the insertion of our molecules aside the Zn loop disturbs the interface of the dimer, thus inhibiting the dimerization through an allosteric effect (conformational change). We also hypothesize the 4-NH₂ (donor) may have an H-bond interaction with GLU386, Figure 6A. In our model, **CU-45** cannot interact with GLU386 mainly because there is not a H (donor) on the N-atom and due to steric clash with the methyl groups, see Figure 6B. The in vitro results for **CU-45** and **9** (0% cGAS inhibition) are consistent with our hypothesis. Determining the pK_a values of LYS394 and LYS347 would be useful for probing the electrostatic environment of cGAS and provide insights on how distinct protonation states of ionizable residues impact the enzyme active site. Ongoing efforts include determining how binding affinities of our inhibitors change the protonation states of both native LYS394 and LYS347 as well as the corresponding acylated residues. We provide an estimation of the pK_a values of LYS394 and LYS347 to be ≤ 10.8 since pK_a measurements and calculations are experimentally demanding and difficult.¹³¹ The molecular docking studies also indicate **CU-76** and analogs may bind to different pocket compared to other cGAS inhibitors.¹⁶ Of course, further clarification of the inhibitory mechanism is necessary. Co-crystallizations studies are needed to provide insights on the specific binding mode.

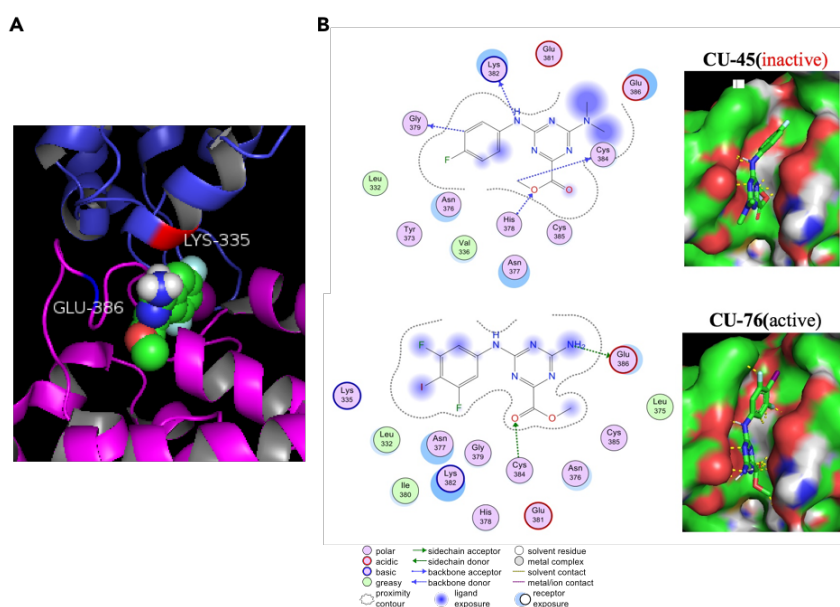


Figure 6. Molecular docking studies for **CU-45** and **CU-76** cGAS inhibitors. (A) Close-up view of the binding site of **CU-76** on the cGAS dimer interface. **CU-76** may potentially disrupt the interface of the mcGAS dimer by inserting aside the Zn loop. (B) Schematic representation of residues around the molecules (left, using MOE v.2014.0901) and close-up view of the binding site on the protein interface (right, using PYMOL v2.0.7) are shown. For **CU-45**, methylation of –NH₂ abrogates H-bond interaction with GLU386. In the right pictures, contacts within 3 Å are shown, See Supplemental Figure S8A and S8B and Supplemental Experimental Procedures.

To rule out disruption of the cGAS-DNA complex as an alternative inhibition mode, we performed electrophoretic mobility shift assay (EMSA) in the presence and absence of **CU-32** and **CU-76**.^{12,13} cGAS protein caused mobility shift of ISD (lane2) and reduction of the unbound DNA. This effect was reversed by adding Quinacrine (lane 2-4), a compound known to disrupt cGAS:DNA binding³², see Supplemental Figure S9. In contrast,

1 either **CU-32** (lane 6-8) or **CU-76** (lane 9-11) had no effect on cGAS-caused shift. This result indicates **CU-32** and **CU-76** do not disrupt cGAS:DNA
2 intercalation.
3

4 CONCLUSION

5 In conclusion, we have successfully discovered and characterized a novel small molecule inhibitor, with a distinct chemical scaffold, targeting
6 hcGAS with high binding affinity in vitro. Our cellular studies indicate **CU-32**, **CU-76**, and analogs selectively inhibit the DNA pathway representing
7 a new class of hcGAS inhibitors with cellular activity in human THP-1 cells. Using mouse and human cell lines, we determined the inhibitory activity
8 of **CU-32** is only specific for hcGAS versus mcGAS in cells. Further studies are needed to gain insights on the cellular activity differences. Lastly,
9 **CU-32** and **CU-76** are selective for the cytosolic DNA pathway over other NA-sensing pathways such as RIG-I-MAVS and endosomal TLRs. In
10 general, our discovered small molecule inhibitors provide a new chemical scaffold for developing hcGAS inhibitors with potential therapeutic appli-
11 cations and a much-needed small molecule chemical probe for studying cGAS biology and cGAS related disorders in human cells.
12
13
14
15
16

17 EXPERIMENTAL SECTION

18 **Virtual screening procedure.** High throughput virtual screening (HTVS) was performed against the cGAS/dsDNA complex structure. The Enamine
19 drug database (1.3 million small molecules) and Maybridge library (50,000 small molecules) was docked into the dsDNA-binding domain of cGAS (PDB:
20 4O6A). Glide maestro protocol was used for the virtual screening using Schrodinger software. The grid was generated on the protein-protein interface with
21 incorporation of important residues involved in dsDNA binding, See Figure 1.
22
23
24

25 The protocol includes addition of hydrogens, restrained energy-minimizations of the protein structure with the Optimized Potentials for Liquid Simula-
26 tions-All Atom (OPLS-AA) force field, and finally setting up the Glide grids using the Protein and Ligand Preparation Module. All compounds were first docked
27 and ranked using High Throughput Virtual Screening Glide, continued with standard precision docking (SP) Glide for the top 10,000 compounds. To reduce
28 the number of compounds in the library, after performing HTVS screening, the remaining 10% was docked using the more accurate and computationally inten-
29 sive SP docking, after which the remaining 10% was docked using Extra-precision. The top ranked compounds were re-ranked by predicted binding energy. The
30 compounds were filtered by Lipinski's rule of five and reactive functionality. It performed docking of the drug compounds in the different phases like HTVS,
31 SP, XP (Extra-precision).
32
33
34
35
36

37 Selection of the candidate molecules was based on four criteria: (1) predicted binding energy and spatial complementarity; (2) reasonable chemical struc-
38 tures found in the dsDNA-binding site of cGAS; (3) existence of at least one hydrogen bond between the ligand and one of the dsDNA-recognizing residues on
39 the cGAS surface; (4) drug-like properties analysis. Drug-like properties follow Lipinski's rule of five and include properties such as molecular weight, hydrogen
40 bond or, hydrogen bond acceptor, Lipophilicity (log P), and human oral absorption. Ten of these molecules were selected by chemical and geometrical proper-
41 ties for experimental evaluation (Table 1).
42
43
44
45

46 **cGAS in vitro assay.** The initial hits and all cGAS inhibitors described herein were evaluated using an in vitro cGAS assay. Briefly, serial dilutions of
47 compounds in DMSO were added to a reaction mixture containing 20mM Tris-Cl, 5mM MgCl₂, 0.2mg/ml bovine serum albumin (BSA), 0.01mg/ml Herring
48 testis DNA (HT-DNA), 0.1mM GTP, 0.006mM ATP, and 30nM human cGAS protein, incubated at 37°C for 20min. Remaining ATP levels was measured by
49 adding 40µl of KinaseGlo (Promega) and reading luminescence. Reactions omitting cGAS and reactions without compounds but DMSO were considered
50 100% and 0% inhibition, respectively. IC₅₀ values were deduced from non-linear fitting of [inhibitor] vs response in Prism 8.
51
52
53
54
55
56
57
58
59
60

Fluorescence polarization assay (FP) for DNA intercalations studies. Select target compounds from structure activity relationship analysis (SAR) studies were tested in a fluorescence polarization (FP) assay for their ability to intercalate DNA following the protocol developed for known cGAS inhibitors.^{12a} The assay was performed in a final volume of 30 μL in 384-solid bottom opaque plates. Ten microliters of HEN buffer (10mM HEPES pH 7.5, 1mM EDTA pH 7.5, 100mM NaCl) were dispensed per well using an Eppendorf multichannel pipette. Compounds were dissolved in DMSO and dispensed per well (10 μL dosing volume) using Eppendorf multichannel pipette. Ten microliters of a solution of 150 nM acridine orange in HEN buffer was dispensed per well using Eppendorf multichannel pipette. Subsequently, 10 μL of a solution of 45-bp dsDNA at μgml^{-1} , see Supplemental Table S5, was dispensed per well using Eppendorf multichannel pipette. The liquid was collected at the well bottom using centrifugation for 30 s at 180 x g. Mitoxantrone, a known DNA intercalator, was used at 50 μM as a positive control, while DMSO alone was used as negative control. FP was measured using a Synergy H2 plate reader. The data was analyzed and plotted using Microsoft Excel.

Secreted embryonic alkaline phosphatase (SEAP) assay. Cell Culture and SEAP Assay: Commercially available human embryonic kidney (HEK) 293 cells expressing human Toll-like receptor (hTLR) gene and an inducible secreted embryonic alkaline phosphatase (SEAP) reporter gene were used to evaluate compound potency on TLR pathways. The SEAP reporter gene is fused to five NF- κB and AP-1 sites. Stimulation of the hTLR is induced with natural ligand or small molecule chemical ligand (R848, Invivogen). This activates NF- κB and AP-1, which induces the production of SEAP protein. Growth media for cell maintenance was prepared using DMEM media with 10% FBS, 1% L-glutamine, 1% Penicillin/Streptomycin and supplemental antibiotics (10 $\mu\text{g}/\text{mL}$ blasticidin and 100 $\mu\text{g}/\text{mL}$ zeocin) per manufacture's recommendations.

Un-supplemented test media was prepared using DMEM media with 10% FBS (deactivated), 1% L-glutamine, and 1% Penicillin/Streptomycin (Note: supplemental antibiotics were not added). 100,000 cells/well or 70,000 cells/well were plated in a tissue culture treated 96-well (Costar 3596) in un-supplemented DMEM test media. Cells were then treated with appropriate concentration of compound, natural TLR ligand (5 $\mu\text{g}/\text{mL}$ Poly(I:C), 20 ng LPS, 1 $\mu\text{g}/\text{mL}$ R848, 1 $\mu\text{g}/\text{mL}$ CpG-ODN, or ssRNA/LyoVec, (Invivogen). The cells were incubated for 18–20 hours and assayed for NF- κB signaling using a SEAP assay. Quanti-Blue (Invivogen) medium for quantification of alkaline phosphatase was used to monitor expression of SEAP via detection of SEAP reporter protein secreted by cells. The compounds were considered active if they decreased SEAP levels as indicated by a decrease in absorbance at 620 nm. The data was normalized as $[(\text{raw data} - \text{untreated cells}) / (\text{ligand} + \text{solvent control} - \text{untreated cells})]$. Ligand + solvent is 100% activation, and untreated cells are 0% activation. The result of one representative biological replicate for three independent days is plotted with the error bars representing the standard deviation of three technical replicates for one independent biological replicate. The result of one representative biological replicate for three independent days is plotted with the error bars representing the standard deviation of three technical replicates for one independent biological replicate.

Nitric oxide (NO) assay. Raw 264.7 cells were plated on day one at 375,000 cells/mL in a tissue culture treated 96-well plate. The cells were plated in supplemented RPMI medium (10% fetal bovine serum, 1% L-glutamine, 1% Penicillin/Streptomycin) and incubated at 37 $^{\circ}\text{C}$. On day two, supplemented media was removed from the cells, and the un-supplemented RPMI was added (100 μL). The cells were treated with 1 $\mu\text{g}/\text{mL}^{-1}$ R848 (90 μL) (Invivogen) and varying concentrations of the appropriate organic compound (10 μL). The final volume in each well was 200 μL . The 96-well plate was incubated with the organic compound for 18–24 hours at 37 $^{\circ}\text{C}$.

On day three, a solution of 0.05 mg/mL^{-1} 2,3-diaminonaphthalene (DAN, Sigma Aldrich) in 0.62 M HCl was prepared. The 96-well plate was removed from the incubator and 90 μL of media from each well was transferred to a black 96-well plate (ThermoScientific), respectively. Followed by the addition of DAN/HCl solution (10 $\mu\text{L}/\text{well}$) each well with. The plate was covered with aluminum foil and shaken at room temperature for 15–20 minutes. The plate was

quenched with 3 M aqueous NaOH (5 μL / well). A BioTek Synergy HTX Multi-mode reader or a Beckman Coulter DTX 880 Multimode Detector were used to quantify the results. Samples were excited at 360 nm and emission was measured at 430 nm. The data was normalized as (well raw data – untreated cells)/(ligand + solvent control – untreated cells) such that ligand + solvent is 100% activation, and untreated cells are 0% activation. The experiment was conducted with a minimum of three biological replicates, in triplicate.

The NO assay uses an aryldiazonium intermediate to convert 2,3-diaminonaphthalene to fluorescent 1(H)-naphthotriazole in the presence of NO. As NO is produced in the TLR inflammatory response, this readout provides information on the extent of TLR signaling.

Cell culture and interferon regulatory factor (IRF)-Lucia assay. Commercially available Raw-Dual cells (Invivogen) transfected with IRF-Luc/KI-[macrophage inflammatory protein-2 (MIP-2)]-secreted embryonic alkaline phosphatase (SEAP) reporter genes and an inducible Lucia luciferase gene (Luc) were used to evaluate compound potency for murine macrophages. The Lucia luciferase gene is under the control of an ISG54 minimal promoter with IFN-stimulated response elements. Stimulation of cGAS was induced with G3YSD, a cGAS agonist (Invivogen). This activates the IRF pathway, which induces the production of the Luciferase protein. Growth media for cell maintenance was prepared using DMEM media with 10 % FBS 1% L-glutamine, 1% Penicillin/Streptomycin and supplemental antibiotics (100 $\mu\text{g}\text{mL}^{-1}$ normocin and 200 $\mu\text{g}\text{mL}^{-1}$ zeocin) per manufacture's recommendations to select for cGAS and IRF-Lucia/KI-[MIP-2]SEAP reporter expression.

Un-supplemented test media was prepared using DMEM media with 10% FBS (heat deactivated), 1% L-glutamine, and 1% Penicillin/Streptomycin (Note: supplemental antibiotics were not added). 100,000 cells/well were plated in a tissue culture treated 96-well (Costar 3596) in un-supplemented DMEM test media. Cells were then treated with appropriate concentration of compound, and 1 $\mu\text{g}\text{mL}^{-1}$ G3YSD ligand. The cells were incubated for 18–20 hours and assayed for IRF signaling using a Lucia luciferase assay. Quantit-Luc (Invivogen) medium for quantification of luciferase was used to monitor the expression of luciferase via detection of Lucia luciferase reporter protein secreted by cells. The compounds were considered active if they decreased luciferase levels as indicated by a decrease in luminescence relative light units (RLU). The data was normalized with 100% untreated cells as the negative control and 100% cells treated with cGAS ligand (1 $\mu\text{g}\text{mL}^{-1}$ G3YSD) as the positive control. All data for cell-based assays is represented as the average and standard deviation of three biological replicates, unless otherwise noted.

Molecular docking calculations for cGAS inhibitors. The crystal structure of murine cGAS (mcGAS) –DNA(2:2) complex (PDB: 4O6A) was used. Similar to the approach described above for the HTVS, we processed 4O6A prior to docking and only the monomer mcGAS was retained. The DNA and water molecules were removed. The compounds were first optimized using the GaussView v.5.0.9 and Gaussian v.9.5 (Method: b3lyp, Basic set: 6-31+g(d,p), pseudo potential for I: sdd). We prepared the ligands and protein receptor with AutoDockTools-1.5.6 (added hydrogens and gasteiger charges, set rotatable bonds for ligands etc.). The GridBox was generated at the cGAS-cGAS interface, Zn loop (K382 E386) and α 7 helix(K335) involved (Supplemental Figure S8A.). The docking parameters were all set to default (Number of Genetic Algorithm Runs: 50). In the first-round of docking, the protein structure was set to be rigid. We then selected one reasonable candidate pose from the results based on the predicted binding energy and spatial complementarity. To further improve docking accuracy, redocking was conducted with select residues (Lys335, Lys382, Glu386) in the GridBox being flexible. Using the docking results, CU-76 was overlapped with mcGAS–DNA(2:2) complex together (Supplemental Figure S8B.).

Quantification and statistical analysis. Statistical differences were performed using one-way ANOVA with the Turkey method for comparisons of experimental group against the control group. All statistical analysis was performed using OriginPro, and a P value of < 0.05 was considered statistically significant.

General Chemical Synthesis Considerations

Unless otherwise noted, all non-aqueous reactions were run under an atmosphere of dried nitrogen in dried glassware. All reagents were reagent grade and used without further purification. Moisture sensitive reagents were added via syringe. All chemicals were obtained from Sigma-Aldrich, Acros, or Strem unless otherwise noted. Flash column chromatography was performed using EM Reagents Silica Gel 60 (230-400). Analytical thin-layer chromatography (TLC) was performed using EM Reagents 0.25 mm silica gel 254-F plates. Visualization was accomplished with UV light, p-anisaldehyde stain, and/or iodine.

^1H NMR and ^{13}C NMR spectra were recorded on Bruker 400 MHz Fourier transform NMR spectrometer. Chemical shifts are reported relative to the solvent resonance peak δ 7.27 (CDCl_3), 3.31 (CD_3OD), and 2.51 (DMSO-d_6) for ^1H and δ 77.23 (CDCl_3), 49.15 (CD_3OD), and 39.51 (DMSO-d_6) for ^{13}C NMR. The ^{13}C NMR spectra were recorded at 101 MHz in CDCl_3 , CD_3OD , or DMSO-d_6 as the internal standards, respectively. Data are reported as follows: chemical shift, multiplicity (s = singlet, d = doublet, t = triplet, q = quartet, bs = broad singlet, m = multiplet), coupling constants, and number of protons. Mass spectrometry was performed at the mass-spectrometry facility of the Biofrontiers Institute at the University of Colorado Boulder. High resolution mass spectra were obtained using a Waters Synapt G2 QToF HR-MS using an ESI ionization mode. Infrared spectra are reported in cm^{-1} and recorded using a Agilent Cary 630 FT/IR instrument and optical rotations were measured on JASCO P-1030 and are reported as an average of data points. The compounds were purified using flash column chromatography (ACI systems, Biotage). Unless otherwise noted, all yields refer to isolated yields, and product purity was determined by ^1H NMR spectroscopy and Agilent HPLC 1200 series instrument with an Eclipse XDB-C₁₈ column. All samples tested were > 95% pure based on HPLC and/or ^1H NMR analysis.

Note: Characterization and spectral data for the intermediates used for the synthesis of inhibitors are described after characterization data for the inhibitors described in the main text.

Numbering System

The numbering system described below has been used in the Supplementary Information and article for NMR assignments and discussion of 1,3,5-triazine derivatives.

General Procedure B: Preparation of arylbiguanide hydrochloride salt:^{19, 27, 28}

Dicyandiamide (0.1 mmol) and the corresponding aniline (0.1 mmol) were weighed into a microwave vial followed by the addition of 3 M HCl. The vial was sealed with a microwave cap and stirred at rt for 24-36 hours. The arylbiguanide hydrochloride salt was filtered and washed with cold H_2O (3 x 5 mL). The arylbiguanide hydrochloride salts were used without further purification or were purified by trituration with Et_2O or MeOH. All salts were characterized by HRMS and/or ^1H NMR. Note: For previously synthesized arylbiguanide hydrochloride salts, only the characterization data for the corresponding 4-amino-1,3,5-carboxylates is provided. Characterization data for all new arylbiguanide hydrochloride salts and the corresponding 4-amino-1,3,5-carboxylates is included herein.

General Procedure C: Preparation of arylbiguanide free base:²⁰

The arylbiguanide salt (1.0 mmol) in anhydrous ethanol or methanol (4.4 M) was added to a mixture of sodium ethoxide (1.2 mmol) in anhydrous ethanol (0.34 M). After stirring the solution for 3 h at rt, the mixture was filtered through a pad of celite. The filtrate was concentrated by rotary evaporation. The residue was dissolved in hot ethanol and filtered through a pad of celite. The filtrate was concentrated by rotary evaporation to afford the desired arylbiguanide base and was used without further purification.

General Procedure D: Preparation of 4-amino-1,3,5-carboxylates:²⁰

Dimethyl oxalate (3.0 mmol) was added to the arylbiguanide base in anhydrous MeOH (0.27 M). After stirring the solution at 35 °C for 1 h, the solution was heated to reflux and stirred overnight. The reaction mixture was cooled to rt and allowed to stand for 3 h. The crystals were collected by filtration, washed with cold methanol, and dried under vacuum. The solid was recrystallized with hot methanol (or isopropanol) or chromatographed to afford the product as crystalline solids.

Methyl 4-amino-6-((4-fluorophenyl)amino)-1,3,5-triazine-2-carboxylate (1)²⁰: Following the general free base procedure C, a mixture of 1-carbamimidamido-N-(4-fluorophenyl)methanimidamide hydrochloride (400 mg, 1.73 mmol) and NaOEt (118 mg, 1.73 mmol) was stirred in EtOH (0.34 M) at rt for 3 h. Following the general procedure D, a mixture of dimethyl oxalate (538 mg, 5.19 mmol) and the arylbiguanide base in anhydrous MeOH (0.27 M) was stirred at 25 °C for 3 h and then refluxed overnight. The mixture was cooled to rt and the precipitate was collected by filtration. The solid was recrystallized with isopropanol and stored at -20 °C for 5 d to afford a white solid (231 mg, 97% pure) in 51% yield: m.p. = 226–227 °C; ¹H NMR (DMSO-*d*₆, 400 MHz) δ 10.5 (br, 1H), 7.78 (m, 2H), 7.62 (m, 1H), 7.49 (m, 1H), 7.13 (t, *J* = 8.9 Hz, 2H), 3.82 (s, 3H); ¹³C{¹H} NMR (DMSO-*d*₆, 101 MHz) δ 167.2, 164.2, 164.0, 163.9, 158.7 (d, ¹*J*_{CF} = 239.2 Hz), 135.8 (d, ⁴*J*_{CF} = 2.5 Hz), 121.7 (d, ³*J*_{CF} = 3.2 Hz), 115.1 (d, ²*J*_{CF} = 22.0 Hz), 52.5; ¹⁹F NMR (DMSO-*d*₆, 365 MHz) δ -121.0; IR (film) ν 3238 3096, 1748, 1644, 1212, 787; HRMS (ESI-TOF) *M/z*: *m/z*: [M+H]⁺ Calcd for C₁₁H₁₁FN₅O₂ 264.0897; Found 264.0894.

General procedure A for lithium aluminum hydride (LiAlH₄) reduction:

(4-Amino-6-((4-fluorophenyl)amino)-1,3,5-triazin-2-yl)methanol (2a): To a solution of methyl 4-amino-6-((4-fluorophenyl)amino)-1,3,5-triazine-2-carboxylate (250 mg, 0.950 mmol) in anhydrous THF (2.0 mL) was added dropwise to a slurry of LiAlH₄ in anhydrous THF (9.5 mL) under a N₂ atmosphere. After stirring the mixture at rt for 3 h, the reaction was quenched utilizing the Fieser protocol. The mixture was diluted with diethyl ether and cooled to 0 °C. Water (0.250 mL) was slowly added to the mixture and allowed to stir for 5 minutes. Next, 15% aqueous NaOH (0.250 mL) was added followed by water (3 x 0.75 mL) and then stirred for 15 min. Sodium sulfate was added and the mixture was stirred for another 15 min, filtered, and concentrated by rotary evaporation to afford a white solid (4%, 97% pure; Note: LiBH₄ and NaBH₄ can also be used, 15 and 63-77% yield respectively): m.p. = 223-224 °C; ¹H NMR (DMSO-*d*₆, 400 MHz) δ 9.59 (br, 1H), 7.79 (dd, *J* = 10.5, 5.0 Hz, 2H), 7.10 (*J* = 8.9 Hz, 2H) 7.10 (br s, 2H), 4.86 (t, *J* = 6.1 Hz, 1H), 4.21 (d, *J* = 6.1 Hz, 2H); ¹³C{¹H} NMR (DMSO-*d*₆, 101 MHz) δ 177.0, 166.6, 164.0, 157.4 (d, ⁴*J*_{CF} = 238.6 Hz), 136.3 (³*J*_{CF} = 2.6 Hz), 121.4 (²*J*_{CF} = 7.6 Hz), 114.9 (¹*J*_{CF} = 238 Hz), 63.8; IR (film) ν 3499, 3324, 3134, 1670, 1555, 1506, 1212, 1093, 825; ¹⁹F NMR (DMSO-*d*₆, 365 MHz) δ -121.8; HRMS (ESI-TOF) *m/z*: [M+H]⁺ Calcd for C₁₀H₁₁FN₅O, 236.0944; Found 236.0948.

N2-(4-Fluorophenyl)-6-(methoxymethyl)-1,3,5-triazine-2,4-diamine (2b): The general procedure was followed using 1-carbamimidamido-N-(4-fluorophenyl)methanimidamide hydrochloride (1.83 g, 7.9 mmol), NaOMe (513 mg, 9.5 mmol), and in anhydrous MeOH (23 mL). The corresponding arylbiguanide base, ethylmethoxyacetate (0.95 mL, 8.06 mmol), and 15 mL MeOH were added and then heated at reflux for 24 h. The reaction mixture was cooled to rt and concentrated to afford a white solid. The solid was purified by column chromatography (1–5% MeOH:CH₂Cl₂) to afford a white solid (75 mg, 97% pure) in 4% yield: m.p. = 185–188 °C; ¹H NMR (DMSO-*d*₆, 400 MHz) δ 9.60 (s, 1H), 7.80 (dd, *J* = 9.1, 5.0 Hz, 2H), 7.10 (t, *J* = 8.9 Hz, 2H), 7.10 (overlapping br s, 2H), 4.18 (s, 2H), 3.36 (s, 3H); ¹³C{¹H} NMR (DMSO-*d*₆, 101 MHz) δ 174.4, 166.7, 164.1, 157.4 (d, ¹*J*_{CF} = 238.7 Hz), 136.2 (d, ⁴*J*_{CF} = 2.4 Hz), 121.4 (d, ³*J*_{CF} = 7.5 Hz), 114.9 (d, ²*J*_{CF} = 22.0 Hz), 73.8, 58.2; ¹⁹F NMR (DMSO-*d*₆, 365 MHz) δ -121.3; IR (film) ν 3353, 3160, 1201, 1119; HRMS (ESI-TOF) *m/z*: [M+H]⁺ Calcd for C₁₁H₁₃FN₅O 250.1099; Found 250.1103.

6-((Aminomethyl)-N2-(4-fluorophenyl)-1,3,5-triazine-2,4-diamine (2c): Following the general procedure A using 4-amino-6-((4-fluorophenyl)amino)-1,3,5-triazine-2-carboxamide (240 mg, 0.967 mmol) and LiAlH₄ (110 mg, 2.90 mmol) in anhydrous THF (0.1 M). the reaction was stirred at rt and monitored by TLC. After 6.5 h, the reaction was quenched using the Feiser protocol to afford a yellow residue. The residue was purified using column chromatography (1–5% MeOH:CH₂Cl₂) to afford a white residue (81 mg, 95% pure) in 23–36% yield (Note: Heating the reaction > rt leads to reduction of amine to afford N2-(4-fluorophenyl)-6-methyl-1,3,5-triazine-2,4-diamine and/or decomposition byproducts. At rt, baseline decomposition is observed by TLC. For this reason, the reaction should not be stirred > 7 h at rt. The yields vary significantly between reactions. Additionally, reduction of the corresponding azide derivative using H₂ Pd/C at rt for 1 h affords N2-(4-fluorophenyl)-6-methyl-1,3,5-triazine-2,4-diamine instead of 1c in quantitative yields.): ¹NMR (DMSO-d₆, 400 MHz) δ 9.59 (s, 1H), 7.80 (dd, *J* = 8.9, 5.1 Hz, 2H), 7.10 (t, *J* = 8.7 Hz, 4H), 4.87 (t, *J* = 6.0 Hz, 2H), 4.21 (d, *J* = 5.9 Hz, 2H); ¹³C{¹H} NMR (DMSO-d₆, 101 MHz) δ 176.9, 166.5, 163.9, 156.1 (¹*J*_{CF} = 239.1 Hz) 136.2 (⁴*J*_{CF} = 2.3 Hz), 121.2 (d, ³*J*_{CF} = 7.4 Hz), 114.7 (d, ²*J*_{CF} = 21.9 Hz); ¹⁹F NMR (DMSO-d₆, 365 MHz) δ -121.9; IR (film) *ν* 3547, 3428, 1718, 1502, 1204; HRMS (ESI-TOF) *m/z*: [M+H]⁺ Calcd for C₁₀H₁₂FN₆ 235.1102; Found 235.1107.

Methyl 4-(dimethylamino)-6-((4-fluorophenyl)amino)-1,3,5-triazine-2-carboxylate (8): 4-(Dimethylamino)-6-((4-fluorophenyl)amino)-1,3,5-triazine-2-carbonitrile (37 mg, 0.143 mmol) was added to a flame dried round bottom flask fitted with a reflux condenser. Anhydrous methanol (0.317 mL) was added to the reaction vessel followed by the addition of BF₃•OEt₂ (0.572 mmol). The reaction mixture was refluxed overnight and a white precipitate. The reaction mixture was cooled to ambient temperature and concentrated by rotary evaporation. The residue was re-dissolved in CH₂Cl₂ and washed with H₂O. The organic mixture was dried with Na₂SO₄, filtered, and concentrated by rotary evaporation to afford a white solid. The solid was purified by flash column chromatography (100% CH₂Cl₂ – 5% MeOH:CH₂Cl₂) to afford a white solid (19 mg, 95% pure) in 45% yield: ¹H NMR (DMSO-d₆, 400 MHz) δ 9.55 (s, 1H), 7.77 – 7.71 (m, 2H), 7.52 (br, 2H), 7.13 (td, *J* = 9.1, 2.5 Hz, 2H), 3.84 (s, 3H), 3.16 – 3.08 (m, 6H); ¹³C{¹H} NMR (DMSO-d₆, 101 MHz) δ 159.9, 155.7, 154.7, 154.3, 145.7 (¹*J*_{CF} = 211.5 Hz) 125.8, (⁴*J*_{CF} = 2.4 Hz), 110.9, (³*J*_{CF} = 7.0 Hz), 104.5 (²*J*_{CF} = 22.1 Hz), 43.1, 25.5 (d); ¹⁹F NMR (DMSO-d₆, 365 MHz) δ -121.3; IR (film) *ν* 3408, 1659, 1003; HRMS (ESI-TOF) *m/z*: [M+H]⁺ Calcd for C₁₃H₁₅FN₅O₂ 292.1205; Found 292.1210.

Methyl 4-[(4-fluorophenyl)amino]-6-(methylamino)-1,3,5-triazine-2-carboxylate (9): 4-[(4-Fluorophenyl)amino]-6-(methylamino)-1,3,5-triazine-2-carbonitrile (0.614 mmol) was weighed into a flame dried round bottom flask and dissolved with anhydrous MeOH (0.25 M). Then freshly distilled BF₃OEt₂ (4.91 mmol) was added and refluxed. After 12 h, the mixture was cooled to rt and diluted with H₂O (2 mL). The mixture was extracted with CH₂Cl₂ (3 x 5 mL). The organic mixture was dried with Na₂SO₄, filtered, and concentrated by rotary evaporation to afford a solid. The solid was chromatographed (1-20% MeOH:CH₂Cl₂) to afford a white solid (39 mg, 96% pure) in 23% yield: m.p. = 151–152 °C; ¹H NMR (DMSO-d₆, 400 MHz) δ 9.55 (s, 1H), 7.89 – 7.68 (m, 2H), 7.43 (s, 1H), 7.20 – 6.98 (m, 2H), 3.83 (d, *J* = 16.7 Hz, 3H), 2.81 (dd, *J* = 12.7, 4.7 Hz, 3H); ¹³C{¹H} NMR (DMSO-d₆, 101 MHz) δ 170.5 (d, ³*J*_{CF} = 39.2 Hz), 167.2, 164.9, (d, ²*J*_{CF} = 48.2 Hz), 157.4 (d, ¹*J*_{CF} = 238.6 Hz), 121.4 (d, ⁴*J*_{CF} = 7.3 Hz), 144.9 (d, ³*J*_{CF} = 22.1 Hz), 114.8 (d, ³*J*_{CF} = 22.0 Hz), 53.5, 27.3 (d); ¹⁹F NMR (DMSO-d₆, 365 MHz) δ -122.0; HRMS (ESI-TOF) *m/z*: [M-H]⁻ Calcd for C₁₂H₁₁FN₅O₂ 276.0897; Found 276.0900.

6-((4-Fluorophenyl)amino)pyrimidine-4-carboxylic acid (10): General pyrimidine synthesis procedure was followed using pyrimidine-4-carboxylate (209 mg, 1.21 mmol) and 4-fluoroaniline (0.116 mL, 1.21 mmol) in 2-propanol (2.0 mL, 0.58 M) and 37% HCl (2.18 mmol, 0.214 mL). The reaction was stirred at 100 °C for 19 h. The product hydrolyzed quantitatively to the corresponding carboxylic acid. Purification by column chromatography (eluent 10% MeOH:CH₂Cl₂) provided 5 (157 mg, 92% pure) in 52% yield as a yellow solid: m.p. = 226–227 °C; ¹H NMR (DMSO-d₆, 400 MHz) δ 11.33 (s, 1H), 8.82 (d, *J* = 0.9 Hz, 1H), 7.76 (dd, *J* = 9.0, 4.9 Hz), 7.51 (s, 1H), 7.36 – 7.19 (m, 2H), 3.88 (3H); ¹⁹F NMR (DMSO-d₆, 365 MHz) δ 119.5; HRMS (ESI-TOF) *m/z*: [M-H]⁻ Calcd for C₁₁H₇FN₂O₂ 232.0522; Found 232.0523.

To a solution of 6-((4-fluorophenyl)amino)pyrimidine-4-carboxylic acid in anhydrous methanol was added concentrated H₂SO₄ (20 μL). The resulting mixture was heated at reflux overnight. The mixture was concentrated by rotary evaporation, and the residue was purified by flash column chromatography (5% MeOH:CH₂Cl₂) to afford methyl 6-((4-fluorophenyl)amino)pyrimidine-4-carboxylate (**5**) (46 mg, 95% pure) in 43% yield as a white solid: ¹H NMR (DMSO-d₆, 400 MHz) δ 10.02 (s, 1H), 8.77 – 8.66 (m, 1H), 7.72 (dd, *J* = 9.0, 4.9 Hz, 2H), 7.37 (d, *J* = 1.2 Hz, 1H), 7.30 – 7.12 (m, 2H), 3.88 (s, 3H); ¹³C{¹H} NMR (DMSO-d₆, 101 MHz) δ 164.7, 161.0, 158.0 (d, ¹*J*_{CF} = 239.3 Hz), 158.5, 152.6, 135.5 (d, ⁴*J*_{CF} = 2.4 Hz), 122.0 (d, ³*J*_{CF} = 7.9 Hz), 115.5 (d, ²*J*_{CF} = 22.4 Hz), 107.7, 52.7; ¹⁹F NMR (DMSO-d₆, 365 MHz) δ -119.5; IR (film) ν 3324, 1566, 843; HRMS (ESI-TOF) *m/z*: [M+H]⁺ Calcd for C₁₂H₁₁FN₃O₂ 248.083; Found 248.0837.

Methyl 3-amino-5-((4-fluorophenyl)amino)benzoate (11): A mixture of methyl 3-((4-fluorophenyl)amino)-5-nitrobenzoate (**44**) (150.1 mg, 0.517 mmol) and 10 mol% Pd/C (1.7 mg, 0.0517 mmol) in anhydrous methanol (3.7 mL, 0.14 M) was stirred at rt under 1.1 atm of H₂ for 12 h. The reaction progress was monitored by TLC using 5% MeOH:CH₂Cl₂. After 12 h, the catalyst was removed by filtration using Celite® and methanol. The filtrate was concentrated by rotary evaporation to afford a brown solid. The solid was purified using column chromatography (1–5% MeOH:CH₂Cl₂) to afford a light brown solid (92 mg, 99%) 54% yield: m.p. = 135–136 °C; ¹H NMR (DMSO-d₆, 400 MHz) δ 8.01 (br, 1H), 7.07 (d, *J* = 8.5 Hz, 2H), 7.05 (d, *J* = 5.0 Hz, 2H), 7.76 (dd, *J* = 3.6, 1.6 Hz, 1H), 6.61 (dd, *J* = 3.5, 1.6 Hz, 1H), 6.47 (t, *J* = 2.1 Hz, 1H), 5.28 (br, 2H) 3.75 (s, 3H); ¹³C{¹H} NMR (DMSO-d₆, 101 MHz) δ 166.9, 156.5 (d, ¹*J*_{CF} = 236.3 Hz), 149.8, 145.0, 139.5 (d, ⁴*J*_{CF} = 2.0 Hz), 130.8, 119.6 (d, ³*J*_{CF} = 7.7 Hz), 115.7 (d, ²*J*_{CF} = 22.2 Hz), 106.4, 104.9, 104.8, 51.8; ¹⁹F NMR (DMSO-d₆, 365 MHz) δ -123.5; IR (film) ν = 3413, 3435, 1711, 1506, 1219, 769, 521; HRMS (ESI-TOF) *m/z*: [M+H]⁺ Calcd for C₁₄H₁₄FN₂O₂ 261.1034; Found 261.1039.

Methyl 4-amino-6-((4-fluorophenyl)amino)picolinate (12): A mixture of methyl 6-((4-fluorophenyl)amino)-4-nitropicolinate (**46**) (16.0 mg, 0.0549 mmol) and 20 mol% Pd/C (1.2 mg, 0.0110 mmol) in anhydrous methanol (0.8 mL, 0.07 M) was stirred at rt under 1.1 atm H₂ pressure. TLC was used to monitor the reaction progress. (5% MeOH:CH₂Cl₂). After 2 h, the catalyst was removed by filtration using Celite®. The solid residue was washed with methanol and the filtrate was concentrate by rotary evaporation to afford a purple residue. The residue was purified by flash column chromatography (gradients 100% CH₂Cl₂ to 0.5, 1, and 5 % MeOH:CH₂Cl₂) to afford a solid in 71% yield (10.1 mg). ¹H NMR (Methanol-d₄, 400 MHz) δ 7.40 (dd, *J* = 9.2, 4.8 Hz, 2H), 7.04–6.96 (m, 2H), 6.88 (d, *J* = 1.9 Hz, 1H), 6.14 (d, *J* = 1.9 Hz, 1H), 3.87 (s, 3H); ¹³C{¹H} NMR (Methanol-d₄, 101 MHz) δ 167.8, 159.7 (d, ¹*J*_{CF} = 240.1 Hz), 158.9, 158.2, 147.3, 138.9 (d, ⁴*J*_{CF} = 2.6 Hz), 123.0 (d, ³*J*_{CF} = 7.7 Hz), 116.4 (d, ²*J*_{CF} = 22.6 Hz), 106.5, 95.0, 52.8; ¹⁹F NMR (Methanol-d₄, 365 MHz) δ -123.76; HRMS (ESI-TOF) *m/z*: [M+H]⁺ Calcd for C₁₃H₁₃FN₃O₂ 262.0987; Found 262.0993.

Methyl 4-amino-6-((4-fluorophenyl)(methyl)amino)-1,3,5-triazine-2-carboxylate (13): Following the general free base procedure C, a mixture of aryl biguanide salt (**61**) (2.5 g, 10.0 mmol) and NaOEt (885 mg, 13.0 mmol) was stirred in EtOH (0.3 M) at rt for 3 h. Following the general procedure D, a mixture of dimethyloxalate (3.5 g, 30.0 mmol) and the arylbiguanide base in anhydrous MeOH (0.27 M) was stirred at 25 °C for 1h and then refluxed overnight. The mixture was cooled to rt and the crude product was collected by filtration. The crude product was purified with column chromatography (5% MeOH:CH₂Cl₂) to afford a white solid (784 mg, 92% pure) in 50% yield (over two steps): m.p. = 176–178 °C; ¹H NMR (DMSO-d₆, 400 MHz) 7.40 (s, 1H), 7.40 – 7.33 (m, 2H), 7.30 – 7.18 (m, 3H), 3.78 (s, 3H), 3.39 (s, 3H); ¹³C{¹H} NMR (DMSO-d₆, 101 MHz) δ 167.2, 165.9, 164.63, 164.57, 160.5 (d, ¹*J*_{CF} = 243.6 Hz), 140.7 (d, ⁴*J*_{CF} = 2.8 Hz), 129.4 (d, ³*J*_{CF} = 8.6 Hz), 116.1 (d, ²*J*_{CF} = 22.6 Hz) 52.9, 38.5; ¹⁹F NMR (DMSO-d₆, 365 MHz) δ -116.2; IR (film) ν 3517, 3137, 1610, 1510, 1219, 799; HRMS (ESI-TOF) *m/z*: [M+H]⁺ Calcd for C₁₂H₁₃FN₃O₂ 278.1048; Found 278.1051.

(4-Amino-6-((4-fluorophenyl)(methyl)amino)-1,3,5-triazin-2-yl)methanol (14):³⁰ To a solution of methyl 4-amino-6-((4-fluorophenyl)(methyl)amino)-1,3,5-triazine-2-carboxylate, **13**, (500 mg, 1.90 mmol) in anhydrous THF (0.2 M) was added LiBH₄ (1.0 mL, 2.08 mmol) at 0 °C. The

reaction was heated at 50 °C and monitored by TLC. After 12 h, the reaction was quenched with MeOH (1.5 mL) at 0 °C and concentrated to afford a white solid. The crude solid was purified using column chromatography (1–5% MeOH:CH₂Cl₂) to afford the title compound as a white solid (217 mg, 99% pure) in 48% yield: m.p. = 193–195 °C; ¹H NMR (DMSO-d₆, 400 MHz) δ 7.43–7.27 (m, 2H), 7.28–7.09 (m, 2H), 6.92 (s, 2H), 4.65 (t, *J* = 5.9 Hz, 1H), 4.12 (d, *J* = 5.9 Hz, 2H), 3.38 (s, 3H); ¹³C{¹H} NMR (DMSO-d₆, 101 MHz) δ 176.4, 166.4, 165.2, 159.8 (d, ¹*J*_{CF} = 242.5 Hz), 140.7 (d, ⁴*J*_{CF} = 3.1 Hz), 128.9 (d, ³*J*_{CF} = 8.5 Hz), 115.5 (d, ²*J*_{CF} = 22.4 Hz), 63.7, 37.7; ¹⁹F NMR (DMSO-d₆, 365 MHz) δ -116.8; IR (film) ν 3391, 3152, 1670, 1543, 1368, 832; HRMS (ESI-TOF) *m/z*: [M+H]⁺ Calcd for C₁₁H₁₃FN₅O 250.1099; Found 250.1104.

4-Amino-N-benzyl-6-((4-fluorophenyl)amino)-1,3,5-triazine-2-carboxamide (15)³²: A mixture of methyl 4-amino-6-((4-fluorophenyl)amino)-1,3,5-triazine-2-carboxylate (**1**) (0.570 mmol), benzyl amine (0.855 mmol), and 20 mol% (0.114 mmol) glacial acetic acid in dioxane (8 mL) was heated at reflux. The reaction was monitored with TLC (5% MeOH:CH₂Cl₂). After 19 h, the mixture was cooled to rt and concentrated by rotary evaporation. The residue was poured onto ice, and the resulting precipitate was collected by vacuum filtration. The solid was recrystallized from MeOH to afford a white solid in 64% yield (123 mg, 96% pure): m.p. = 243–244 °C; ¹H NMR (DMSO-d₆, 400 MHz) δ 9.94 (s, 1H), 8.79 (t, *J* = 6.3 Hz, 1H), 7.94 – 7.64 (m, 2H), 7.48 – 7.37 (m, 2H), 7.37 – 7.29 (m, 4H), 7.18 – 7.05 (m, 2H), 4.44 (d, *J* = 6.2 Hz, 2H); ¹³C NMR (DMSO-d₆, 101 MHz) δ 167.0, 166.3, 164.3, 163.1, 157.7 (d, ¹*J*_{CF} = 240.1 Hz), 139.0, 135.9 (d, ³*J*_{CF} = 2.6 Hz), 128.4, 127.5, 126.7, 121.7 (m), 115.0 (d, ²*J*_{CF} = 22.2 Hz), 42.4; ¹⁹F NMR (DMSO-d₆, 365 MHz) δ -120.7; IR (film) ν 3491, 3294, 1677, 1629, 1510, 1231, 832; HRMS (ESI-TOF) *m/z*: [M+H]⁺ Calcd for C₁₇H₁₆FN₆O 339.1365; Found 339.1370.

4-Amino-6-((4-fluorophenyl)amino)-N-methyl-1,3,5-triazine-2-carboxamide (16): Methyl-4-amino-6-((4-fluorophenyl)amino)-1,3,5-triazine-2-carboxylate (**1**) (300 mg, 1.14 mmol) was weighed into a glass tube followed by the addition of anhydrous MeOH (0.11 M). Then 0.5 M NH₃ (39.9 mL, 39.9 mmol) in THF was added to the mixture. The glass tube was sealed with a screw cap and heated at 120 °C for 24 h. The reaction mixture was cooled to rt and concentrated by rotary evaporation to afford a white solid. The solid was recrystallized (1:1 petroleum ether:diethyl ether) to afford a white solid in 96% yield (272 mg, 97% pure): m.p. = > 260 °C; ¹H NMR (DMSO-d₆, 400 MHz) δ 9.85 (s, 1H), 7.79 (dd, *J* = 9.0, 5.0 Hz, 2H), 7.67 (br s, 2H), 7.34 (br s, 2H), 7.21 – 7.04 (m, 2H); ¹³C{¹H} NMR (DMSO-d₆, 101 MHz) δ 167.1, 166.5, 164.9, 164.4, 157.6 (d, ¹*J*_{CF} = 239.1 Hz), 135.9 (d, ⁴*J*_{CF} = 2.6 Hz), 121.7 (d, ³*J*_{CF} = 8.7 Hz), 115.0 (d, ²*J*_{CF} = 22.2 Hz); ¹⁹F NMR (DMSO-d₆, 365 MHz) δ -121.3; IR (film) ν 3551, 3435, 1637, 1558; HRMS (ESI-TOF) *m/z*: [M+H]⁺ Calcd for C₁₀H₁₀FN₆O 249.0895; Found 249.0900.

Preparation of cGAS Inhibitors – see General Procedures B, C, and D

Methyl 4-amino-6-(phenylamino)-1,3,5-triazine-2-carboxylate (17): Following the general free base procedure C, a mixture of 1-carbamimidamido-N-phenylmethanimidamide hydrochloride¹ (1.0 g, 4.681 mmol) and NaOEt (318 mg, 4.68 mmol) was stirred in EtOH (0.34 M) at rt for 3 h. Following the general procedure D, a mixture of dimethylxalate (1.6 g, 14.0 mmol) and the arylbiguanide base in anhydrous MeOH (0.27 M) was stirred at 25 °C for 3 h and then refluxed overnight. The mixture was cooled to rt and the precipitate was collected by filtration. The solid was triturated with MeOH to afford a white solid (534 mg, 99% pure) in 46% yield: m.p. = 206–207 °C; ¹H NMR (DMSO-d₆, 400 MHz) δ 9.98 (br, 1H), 7.79 (d, *J* = 8.0 Hz, 2H), 7.60 (br, 1H), 7.47 (br, 1H, NH₂), 7.30 (d, *J* = 7.3 Hz, 1H), 7.27 (d, *J* = 7.4 Hz, 1H), 7.03–6.98 (m, 1H), 3.83 (s, 3H); ¹³C{¹H} NMR (DMSO-d₆, 101 MHz) δ 167.1, 164.3, 163.9, 139.4, 128.5, 122.5, 120.0, 52.5; IR (film) ν 3484, 3350, 1737, 1644, 1242; HRMS (ESI-TOF) *m/z*: [M+H]⁺ Calcd for C₁₁H₁₂N₅O₂ 246.0986; Found 246.0991.

Methyl 4-amino-6-((4-(trifluoromethyl)phenyl)amino)-1,3,5-triazine-2-carboxylate (18): Following the general free base procedure C, a mixture of 1-carbamimidamido-N-[4-(trifluoromethyl)phenyl]methanimidamide¹ hydrochloride (1.3g, 4.75 mmol) and NaOEt (323 mg, 4.75 mmol) was stirred in

MeOH (30 mL) at rt for 22 h. Following the general procedure D, a mixture of dimethyloxalate (1.7 g, 14.3 mmol) and the arylbiguanide base in anhydrous MeOH (0.20 M) was stirred at 35 °C for 1.5 h and then refluxed overnight. The mixture was cooled to rt and the crude product was collected by filtration and washed with cold MeOH. The crude product was recrystallized with MeOH to afford the title compound as a bright yellow solid in 30% yield (450 mg, 97% pure): m.p. = 243–245 °C; ¹H NMR (DMSO-d₆, 400 MHz) δ 10.39 (s, 1H), 8.03 (d, *J* = 8.5 Hz, 2H), 7.82–7.77 (m, 1H), 7.64 (d, *J* = 8.7 Hz, 2H), 3.85 (s, 3H); ¹³C{¹H} NMR (DMSO-d₆, 101 MHz) δ 167.6, 165.0, 164.5, 164.2, 143.7, 126.2 (q, ³*J*_{CF3} = 7.7 Hz), 123.6, 122.7 (d, ²*J*_{CF3} = 32.0 Hz), 120.0, 53.0 two unresolved quartet; ¹⁹F NMR (DMSO-d₆, 365 MHz) δ -60.05; IR (film) ν 3506, 3119, 1748, 1543, 1227, 1111, 791; HRMS (ESI-TOF) *m/z*: [M+H]⁺ Calcd for C₁₂H₁₁F₃N₅O₂ 314.0860; Found 314.0858.

Methyl 4-amino-6-((4-iodophenyl)amino)-1,3,5-triazine-2-carboxylate (19): The general procedure C was followed using 1-carbamimidamido-N-(4-iodophenyl)methanimidamide hydrochloride (**48**) (4.0 g, 11.8 mmol), sodium methoxide (829 mg, 15.34 mmol), and dimethyloxalate (4.2 g, 35.4 mmol) in anhydrous MeOH (35 mL and 20 mL, respectively) at rt to reflux for 24 h. The precipitate was filtered and triturated with MeOH to afford a white solid (1.32 g, 99% pure) in 30% yield: m.p. = 224–225 °C; ¹H NMR (DMSO-d₆, 400 MHz) δ 10.10 (br, 1H), 7.64–7.60 (m, 4H), 7.52 (br s, 1H), 3.83 (s, 3H); ¹³C{¹H} NMR (DMSO-d₆, 101 MHz) δ 167.6, 164.7, 164.4, 164.3, 139.8, 137.5, 122.6, 86.3, 53.0; IR (film) ν 3327, 3182 3327, 1752, 1666, 1536, 1219, 795, 504; HRMS (ESI-TOF) *m/z*: [M+H]⁺ Calcd for C₁₁H₁₁IN₅O₂ 371.9952; Found 371.9959.

4-Amino-6-((4-iodophenyl)amino)-1,3,5-triazine-2-carboxylic acid (19b): Aqueous 1 M NaOH (2.16 mmol) was added to a solution of methyl 4-amino-6-((4-iodophenyl)amino)-1,3,5-triazine-2-carboxylate (**19**) (800 mg, 2.16 mmol) in ethanol (10.8 mL). After heating at reflux for 3 h, the reaction mixture was cooled to rt. Aqueous 1 M HCl (0.540 mL, 4 M HCl in dioxane) was added slowly. The mixture was stirred for 2 h at ambient temperature. After allowing the solution to stand for approximately 30 min, the yellow precipitate was filtered and washed with water and acetone several times. The yellow solid was dried under vacuum to afford 4-amino-6-((4-iodophenyl)amino)-1,3,5-triazine-2-carboxylic acid in (885 mg, 97% pure) in quantitative yield. The product was used without purification: m.p. = 257–258 °C; ¹H NMR (DMSO-d₆, 400 MHz) δ 10.05 (s, 1H), 7.63 (q, *J* = 8.9 Hz, 4H), 7.55–7.19 (m, 1H); ¹³C{¹H} NMR (DMSO-d₆, 101 MHz) δ 166.9, 165.4, 165.0, 164.2, 139.4, 137.0, 122.1, 85.8; IR (film) ν 3320, 3137, 1681, 1491, 1622, 1566, 1331, 776, 631; HRMS (ESI-TOF) *m/z*: [M-H]⁻ Calcd for C₁₀H₇IN₅O₂ 355.9644; Found 355.9645.

Methyl 4-amino-6-((3-iodophenyl)amino)-1,3,5-triazine-2-carboxylate (20): The general procedure C was followed using 1-carbamimidamido-N-(3-iodophenyl)methanimidamide hydrochloride (**49**) (300 mg, 0.883 mmol), NaOMe (62.2 mg, 1.15 mmol), and 2.6 mL in anhydrous MeOH. Following the general procedure D, the corresponding arylbiguanide base, dimethyl oxalate (313 mg, 2.65 mmol) 5.3 mL MeOH at reflux for 12 h. The reaction mixture was cooled to rt and concentrated to afford a grey-purple solid. The solid was purified by column chromatography (1–20% MeOH:CH₂Cl₂) to afford a white solid (154 mg, 92% pure) in 47% yield: m.p. = 212–213 °C; ¹H NMR (DMSO-d₆, 400 MHz) δ 10.10 (s, 1H), 8.14 (s, 1H), 7.89 (s, 1H), 7.71 (s, 1H), 7.58 (s, 1H), 7.36 (dt, *J* = 8.0, 1.1 Hz, 1H), 7.09 (t, *J* = 8.1 Hz, 1H), 3.84 (s, 3H); ¹³C{¹H} NMR (DMSO-d₆, 101 MHz) δ 167.5, 164.7, 163.9, 163.7, 138.9, 133.2, 130.5, 129.3, 119.9, 94.3, 53.8; IR (film) ν 3473, 3149, 1744, 1528, 1219, 1011; HRMS (ESI-TOF) *m/z*: [M+Na]⁺ Calcd for C₁₁H₁₀IN₅O₂Na 393.9777; Found 393.9773.

Methyl 4-amino-6-((2-iodophenyl)amino)-1,3,5-triazine-2-carboxylate (21): The general procedure C was followed using 1-carbamimidamido-N-(2-iodophenyl)methanimidamide hydrochloride (**50**) (400 mg, 1.08 mmol), NaOMe (75.7 mg, 1.40 mmol), and 2.7 mL in anhydrous MeOH. The corresponding arylbiguanide base, dimethyl oxalate (383 mg, 3.24 mmol) 1.8 mL MeOH at reflux 18 h. The reaction mixture was cooled to rt. The solid was precipitated and purified by washing several times with H₂O and Et₂O to afford a white solid (122 mg) in 38% yield: m.p. = 215–216 °C; ¹H NMR (DMSO-d₆, 400 MHz) δ 9.35

(s, 1H, NH), 7.96 – 7.83 (m, 1H), 7.48 – 7.37 (m, 2H), 7.32 (s, 1H), 7.02 (ddd, $J = 7.9, 6.8, 2.2$ Hz, 1H), 3.82 (s, 3H); $^{13}\text{C}\{^1\text{H}\}$ NMR (DMSO- d_6 , 101 MHz) δ 167.6, 165.8, 164.8, 164.5, 140.4, 139.4, 129.3, 129.0, 128.4, 99.7, 52.9; IR (film) ν 3499, 3361, 1741, 1536, 1264, 1007; HRMS (ESI-TOF) m/z : $[\text{M}+\text{H}]^+$ Calcd for $\text{C}_{11}\text{H}_{11}\text{N}_5\text{O}_2$ 371.9957; Found 371.9953.

Methyl 4-amino-6-((4-hydroxyphenyl)amino)-1,3,5-triazine-2-carboxylate (22): The general procedure C was followed using 1-carbamimidamido-N-(4-hydroxyphenyl)methanimidamide hydrochloride (**51**) (700 mg, 3.05 mmol), NaOMe (200 mg, 3.7 mmol), and 7.6 mL in anhydrous MeOH. The corresponding arylbiguanide base, dimethyl oxalate (1.1 g, 9.2 mmol) 10 mL MeOH at reflux 12 h. The solid was precipitated and purified by flash column chromatography (1–20% MeOH: CH_2Cl_2) to afford a white solid (283 mg, 95% pure) in 36% yield: m.p. = 228–229 °C; ^1H NMR (DMSO- d_6 , 400 MHz) δ 9.76 (s, 2H), 9.18 (s, 1H), 7.51 (s, 2H), 7.36 (s, 2H), 6.69 (d, $J = 8.9$ Hz, 2H), 3.82 (s, 3H); $^{13}\text{C}\{^1\text{H}\}$ NMR (DMSO- d_6 , 101 MHz) δ 167.6, 164.5, 164.2, 153.6, 131.2, 122.5, 115.4, 100.0, 52.9; IR (film) ν 3461, 3394, 3163, 1737, 1219, 1022, 638, 612; HRMS (ESI-TOF) m/z : $[\text{M}+\text{Li}]^+$ Calcd for $\text{C}_{11}\text{H}_{11}\text{N}_5\text{O}_3\text{Li}$ 268.1022; Found 268.1029.

Methyl 4-amino-6-((4-methoxyphenyl)amino)-1,3,5-triazine-2-carboxylate (23): Following the general free base procedure C a 1-carbamimidamido-N-(4-methoxyphenyl)methanimidamide hydrochlorideⁱ (200 mg, 0.821 mmol) and NaOEt (67 mg, 0.985 mmol) was stirred in EtOH (0.34 M) at rt for 3 h. Following the general procedure D, a mixture of dimethyloxalate (291 mg, 2.46 mmol) and the arylbiguanide base in anhydrous MeOH (0.27 M) was stirred at 25 °C for 1 h and then refluxed overnight. The mixture was cooled to rt and the precipitate was collected by filtration. The solid was triturated with MeOH to afford a white solid (136 mg) in 60% yield: m.p. = 245–246 °C; ^1H NMR (DMSO- d_6 , 400 MHz) δ 9.86 (br, 1H), 7.64 (br, 2H), 7.52 (1H), 7.40 (br, 1H), 6.86 (d, $J = 9.1$ Hz, 2H), 3.81 (s, 1H), 3.72 (s, 1 H); $^{13}\text{C}\{^1\text{H}\}$ NMR (DMSO- d_6 , 101 MHz) δ 167.2, 164.5, 164.0, 163.8, 155.0, 132.3, 121.7, 113.7, 55.2, 52.4; IR (film) ν 3413, 3160, 1744, 1510, 1223, 1029; HRMS (ESI-TOF) m/z : $[\text{M}+\text{H}]^+$ Calcd for $\text{C}_{12}\text{H}_{14}\text{N}_5\text{O}_3$ 276.1091; Found 276.1096.

Methyl 4-amino-6-((4-ethynylphenyl)amino)-1,3,5-triazine-2-carboxylate (24)³⁴: To a dry THF solution of Methyl 4-amino-6-((4-(trimethylsilyl)ethynyl)phenyl)amino)-1,3,5-triazine-2-carboxylate (45 mg, 0.132 mmol) was added a solution of tetrabutylammonium fluoride (45 mg, 0.172 mmol) dropwise at 25 °C under N_2 . The mixture was stirred at rt and monitored by TLC. After 3.5 h, the mixture was concentrated by rotary evaporation and dissolved with CH_2Cl_2 and washed with H_2O . The organic mixture was dried with Na_2SO_4 , filtered, and concentrated by rotary evaporation to afford a white solid. The solid was purified by flash column chromatography (1–5% MeOH: CH_2Cl_2) to afford a white solid (24 mg, 97% pure) in 61% yield: m.p. = 204–205 °C; ^1H NMR (DMSO- d_6 , 400 MHz) δ 10.20 (s, 1H), 7.85 (d, $J = 8.6$ Hz, 2H), 7.70 (br s, 1H), 7.57 (br s, 1H), 7.47 – 7.29 (d, $J = 9.7$ Hz, 2H), 4.09 (s, 1H), 3.84 (s, 3H); $^{13}\text{C}\{^1\text{H}\}$ NMR (DMSO- d_6 , 101 MHz) δ 167.6, 164.7, 164.4, 164.3, 140.6, 132.6, 120.0, 115.6, 84.3, 80.2, 53.0; IR (film) ν 3327, 3201, 2109, 1744, 1532, 1231, 1011; HRMS (ESI-TOF) m/z : $[\text{M}+\text{H}]^+$ Calcd $\text{C}_{13}\text{H}_{12}\text{N}_5\text{O}_2$ 270.0991; Found 270.0987.

Methyl 4-amino-6-((3,4,5-trifluorophenyl)amino)-1,3,5-triazine-2-carboxylate (25): The general procedure B was followed using 1-carbamimidamido-N-(3,4,5-trifluorophenyl)methanimidamide hydrochloride (**58**) (400 mg, 1.49 mmol), NaOMe (97 mg, 1.79 mmol), and 3.7 mL in anhydrous MeOH. The corresponding arylbiguanide base, dimethyl oxalate (531 mg, 4.5 mmol) 5.0 mL MeOH at reflux 12 h. The solid was precipitated and purified by flash column chromatography (1–20% MeOH: CH_2Cl_2) to afford a white solid (283 mg, 93% pure) in 23% yield: m.p. = 230–232 °C; ^1H NMR (DMSO- d_6 , 400 MHz) δ 10.40 (s, 1H), 7.86 – 7.74 (m, 4H), 3.84 (s, 3H); $^{13}\text{C}\{^1\text{H}\}$ NMR (DMSO- d_6 , 101 MHz) δ 167.1, 164.2, 163.8, 163.6, 151.2 (m, J_{CF}) 148.7 (dd, $^3J_{\text{CF}} = 9.7, 5.7$ Hz), 136.0 (td, $^3a, ^3b, ^4J_{\text{CF}}$ 12.4, 12.2, 3.6 Hz) 132.7 (d, $^1J_{\text{CF}} = 242.9$ Hz), 103.6 (d, $^2bJ_{\text{CF}} = 24.8$ Hz), 52.5; ^{19}F NMR (DMSO- d_6 , 365 MHz) δ -135.0, -135.1; IR (film) ν 3506, 3346, 3301, 1744, 1528, 1029, 791 cm^{-1} ; HRMS (ESI-TOF) m/z : $[\text{M}+\text{H}]^+$ Calcd for $\text{C}_{11}\text{H}_9\text{F}_3\text{N}_5\text{O}_2$ 300.0708; Found 300.0716.

Methyl 4-amino-6-[(3,5-difluoro-4-iodophenyl)amino]-1,3,5-triazine-2-carboxylate (26): The general procedure C was followed using 1-carbamimidamido-N-(3,5-difluoro-4-iodophenyl)methanimidamide hydrochloride (**59**) (65 mg, 0.173 mmol), NaOMe (28 mg, 0.519 mmol), and 0.340 mL in anhydrous MeOH. The corresponding arylbiguanide base, dimethyl oxalate (20.4 mg, 0.173 mmol) 0.340 mL MeOH at reflux for 12 h. The reaction mixture was cooled to rt and concentrated to afford a grey purple solid. The solid was purified by column chromatography (1–20% MeOH:CH₂Cl₂) to afford a white yellow solid (14.3 mg, 96% pure) in 20% yield: ¹H NMR (DMSO-d₆, 400 MHz) δ 7.85 (s, 1H), 7.69 (d, *J* = 9.3 Hz, 2H), 7.24 (br, 2H), 3.84 (s, 3H); ¹³C{¹H} NMR (DMSO-d₆, 101 MHz) δ 170.8, 168.0, 165.2, 163.0 (dd, ¹*J*_{CF} = 239.6 Hz), 160.7, 142.9 (t, ³*J*_{CF} = 14.0 Hz), 102.3 (dd, ²*J*_{CF} = 30.5 Hz), 61.4 (t, ²*J*_{CF} = 31.0 Hz), 53.7; ¹⁹F NMR (DMSO-d₆, 365 MHz) δ -94.0; HRMS (ESI-TOF) *m/z*: [M+H]⁺ Calcd for C₁₁H₉F₂IN₃O₂ 407.9769; Found 407.9778 (+2.2 ppm off).

N²-(4-Iodophenyl)-6-(1,3,4-oxadiazol-2-yl)-1,3,5-triazine-2,4-diamine (27)³⁴: Triethyl orthoformate (0.216 mL) was added to a mixture of FeCl₃ (1.8 mg, 0.011 mmol), L-proline (1.2 mg, 0.011 mmol) and Et₃N (3 μL, 0.022 mmol), and the resulting solution was stirred for 1 h at rt. The hydrazide substrate was added, and the mixture was stirred at 80 °C for 12 h. After cooling, the reaction mixture was washed with Et₂O (3 x 0.5 mL). The organic layer was dried over MgSO₄ and evaporated. The residue was subjected to column chromatography on silica gel (10% MeOH:CH₂Cl₂) to afford a white solid (6 mg) in 29% yield: ¹H NMR (DMSO-d₆, 400 MHz) δ 10.53 (s, 1H), 10.04 (s, 1H), 7.62 (m, 4H); ¹³C{¹H} NMR (DMSO-d₆, 101 MHz) δ 167.3, 166.2, 164.6, 158.7, 139.8, 158.2, 137.5, 122.8, 86.4.

N²-(4-Iodophenyl)-6-(1H-pyrazol-1-yl)-1,3,5-triazine-2,4-diamine (28): Pyrazole (22 mg, 0.317 mmol), 6-chloro-N²-(4-iodophenyl)-1,3,5-triazine-2,4-diamine (100 mg, 0.288 mmol), and K₂CO₃ (44 mg, 0.318 mmol) were weighed into a microwave vial with a stir bar. Anhydrous DMSO (1.0 mL) was added to the sealed vial. The reaction mixture was stirred at 120 °C overnight. The reaction mixture was diluted with EtOAc (5 mL) and 5% aq LiCl (5 x 5 mL). The organic mixture was separated, and the aqueous mixture was extracted with EtOAc (3 x 5 mL). The combined organic mixtures were washed with 5% aq LiCl (5 x 5 mL). The organic mixture was dried with Na₂SO₄, filtered, and concentrated by rotary evaporation to afford a light brown residue. The residue was purified by flash column chromatography (5% MeOH:CH₂Cl₂) to afford a white solid (40 mg, 99% pure) in 46% yield: m.p. = 204–205 °C; ¹H NMR (DMSO-d₆, 400 MHz) δ 9.97 (br s, 1H), 8.50 (dd, *J* = 2.7, 0.7 Hz, 1H), 7.86–7.80 (m, 1H), 7.69 (d, *J* = 8.8 Hz, 2H), 7.63 (d, *J* = 8.9 Hz, 2H), 7.56 (s, 1H), 6.58 (dd, *J* = 2.7, 1.6 Hz, 1H); ¹³C{¹H} NMR (DMSO-d₆, 101 MHz) δ 167.9, 165.2, 162.0, 143.6, 140.0, 137.5, 129.6, 122.7, 109.0, 86.1; IR (film) ν 3324, 3189, 1607, 1394; HRMS (ESI-TOF) *m/z*: [M+H]⁺ Calcd for C₁₂H₁₁IN₇ 380.0121; Found 380.0114.

6-(4-(2-Aminophenyl)-1H-1,2,3-triazol-1-yl)-N²-(4-iodophenyl)-1,3,5-triazine-2,4-diamine (29): 6-Azido-N²-(4-iodophenyl)-1,3,5-triazine-2,4-diamine (**72**) (50 mg, 0.141 mmol) and copper iodide (8.1 mg, 0.042 mmol) were in anhydrous DMSO (0.214 mL) under N₂. After 15 min, 2-ethynyl aniline (48 μL, 0.423 mmol) was added to the mixture and stirred at rt for 2 h. The reaction progress was monitored using TLC until completion. The reaction mixture was diluted with 10% NH₃ aq (1 mL), and the mixture was extracted with EtOAc (3 x 2 mL). The combined organic mixture was washed several times with H₂O and then dried with Na₂SO₄, filtered, and concentrated by rotary evaporation to afford a brown residue. The residue was purified by flash column chromatography (50–75% EtOAc:Hexanes) to afford a white solid (20 mg, 97% pure) in 29% yield: ¹H NMR (DMSO-d₆, 400 MHz) δ 10.25 (broad s, 1H), 8.93 (s, 1H), 7.82 (broad s, 2H), 7.67 (p, *J* = 9.1 Hz, 5H), 7.10 (ddd, *J* = 8.4, 7.2, 1.6 Hz, 1H), 6.82 (dd, *J* = 8.3, 1.2 Hz, 1H), 6.66 (td, *J* = 7.4, 1.2 Hz, 1H), 6.00 (broad s, 2H); ¹³C{¹H} NMR (DMSO-d₆, 101 MHz) δ 165.0, 163.5, 161.0, 146.4, 140.3, 139.7, 137.6, 129.6, 128.0, 123.0, 119.7, 116.8, 113.0, 103.8, 86.7; IR (film) ν 3335, 1607, 1439, 1234; HRMS (ESI-TOF) *m/z*: [M+H]⁺ Calcd for C₁₇H₁₅IN₉ 472.0495; Found 472.0497.

6-(Azidomethyl)-N²-(4-iodophenyl)-1,3,5-triazine-2,4-diamine (30): To a solution of 6-(azidomethyl)-N²-(4-iodophenyl)-1,3,5-triazine-2,4-diamine (**73**) (40 mg, 0.109 mmol) and CuI (6.2 mg, 0.0327 mmol) in DMSO (0.33 mL) was added 2-erthynyl aniline (37.2 μL, 0.327

mmol). The mixture was stirred at rt. After 5 h, the mixture was diluted with brine (1.0 mL) and extracted with EtOAc (2.0 mL X 3). The organic mixture was washed with 5% aq LiCl (2.0 mL). The organic mixture was dried with Na₂SO₄, filtered, and concentrated by rotary evaporation to afford a brown solid. The solid was purified by column chromatography (1–5% MeOH: CH₂Cl₂) to afford a light brown solid (22 mg) in 42% yield: 234–235 °C; ¹H NMR (DMSO-d₆, 400 MHz) δ 9.66 (s, 1H), 8.60 (s, 1H), 7.50 (dd, *J* = 7.8, 1.6 Hz, 1H), 7.46 (br s, 5H), 7.31 (s, 1H), 7.05 (ddd, *J* = 8.4, 7.1, 1.5 Hz, 1H), 6.80 (d, *J* = 8.1 Hz, 1H), 6.61 (ddd, *J* = 8.2, 7.2, 1.2 Hz, 1H), 6.26 (s, 2H), 5.50 (s, 2H); ¹³C{¹H} NMR (DMSO-d₆, 101 MHz) δ 172.4, 167.0, 164.4, 147.9, 146.1, 140.0, 137.3, 128.9, 128.0, 123.4, 122.5, 116.4, 116.2, 113.1, 85.9, 54.5; IR (film) *ν* 3286, 3186, 1618, 1525, 1402; HRMS (ESI-TOF) *m/z*: [M+H]⁺ Calcd for C₁₈H₁₇IN₉ 486.0573; Found 486.0658.

6-(1H-Benzo[d]imidazol-1-yl)-N²-(4-iodophenyl)-1,3,5-triazine-2,4-diamine (31): Benzimidazole (34 mg, 0.288 mmol), 6-chloro-N²-(4-iodophenyl)-1,3,5-triazine-2,4-diamine (100 mg, 0.288 mmol), and K₂CO₃ (51.7 mg, 0.374 mmol) were weighed into a microwave vial with a stir bar. Anhydrous DMSO (0.96 mL) was added to the sealed vial. The reaction mixture was stirred at 120 °C overnight. The reaction mixture was diluted with EtOAc (5 mL) and 5% aq LiCl (5 x 5 mL). The organic mixture was separated, and the aqueous mixture was extracted with EtOAc (3 x 5 mL). The combined organic mixtures were washed with 5% aq LiCl (5 x 5 mL). The organic mixture was dried with Na₂SO₄, filtered, and concentrated by rotary evaporation to afford a light brown residue. The residue was purified by flash column chromatography (5% MeOH:CH₂Cl₂) to afford a white solid (57 mg, 95% pure) in 46% yield: m.p. = > 260 °C; ¹H NMR (DMSO-d₆, 400 MHz) δ 9.90 (broad s, 1H), 8.94 (s, 1H), 8.70 (broad s, 1H), 7.81–7.73 (m, 1H), 7.67 (m, 4H), 7.61 (broad s, 1H), 7.46–7.32 (m, 2H); ¹³C{¹H} NMR (DMSO-d₆, 101 MHz) δ 167.6, 164.8, 162.0, 145.0, 142.0, 139.8, 137.6, 132.0, 124.7, 124.1, 123.0, 120.4, 116.9, 85.6; IR (film) *ν* 3491, 3305, 1547, 1465, 1204; HRMS (ESI-TOF) *m/z*: [M-H]⁻ Calcd for C₁₆H₁₁IN₇ 428.0121; Found 428.0127.

6-(1H-Indol-1-yl)-N²-(4-iodophenyl)-1,3,5-triazine-2,4-diamine (32): Indole (33.7 mg, 0.288 mmol), 6-chloro-N²-(4-iodophenyl)-1,3,5-triazine-2,4-diamine (100 mg, 0.288 mmol), and K₂CO₃ (51.7 mg, 0.374 mmol) were weighed into a microwave vial with a stir bar. Anhydrous DMSO (1.0 mL) was added to the sealed vial. The reaction mixture was stirred at 120 °C overnight. The reaction mixture was diluted with EtOAc (5 mL) and 5% aq LiCl (5 x 5 mL). The organic mixture was separated, and the aqueous mixture was extracted with EtOAc (3 x 5 mL). The combined organic mixtures were washed with 5% aq LiCl (5 x 5 mL). The organic mixture was dried with Na₂SO₄, filtered, and concentrated by rotary evaporation to afford a light brown residue. The residue was purified by flash column chromatography (1% MeOH:CH₂Cl₂) to afford a white solid (35.3 mg, 99% pure) in 29% yield: m.p. = 163–164 °C; ¹H NMR (Methanol-d₄, 400 MHz) δ 8.84 (d, *J* = 8.4 Hz, 1H), 8.19 (d, *J* = 3.7 Hz, 1H), 7.68 – 7.60 (m, 2H), 7.60 – 7.51 (m, 3H), 7.25 (ddd, *J* = 8.4, 7.2, 1.4 Hz, 1H), 7.17 (td, *J* = 7.5, 1.1 Hz, 1H), 6.64 (dd, *J* = 3.8, 0.7 Hz, 1H); ¹³C{¹H} NMR (Methanol-d₄, 101 MHz) δ 169.4, 166.5, 164.8, 141.0, 138.7, 137.0, 132.9, 126.6, 124.5, 124.0, 123.2, 121.7, 118.4, 107.7, 86.3; IR (film) *ν* 3487, 3260, 1607, 1555, 1450, 1216; HRMS (ESI-TOF) *m/z*: [M-H]⁻ Calcd for C₁₇H₁₂IN₆ 427.0168; Found 427.0204.

6-(1H-Indazol-1-yl)-N²-(4-iodophenyl)-1,3,5-triazine-2,4-diamine (33): Indazole (34 mg, 0.288 mmol), 6-chloro-N²-(4-iodophenyl)-1,3,5-triazine-2,4-diamine (100 mg, 0.288 mmol), and K₂CO₃ (44 mg, 0.318 mmol) were weighed into a microwave vial with a stir bar. Anhydrous DMSO (1.0 mL) was added to the sealed vial. The reaction mixture was stirred at 120 °C overnight. The reaction mixture was diluted with EtOAc (5 mL) and 5% aq LiCl (5 x 5 mL). The organic mixture was separated, and the aqueous mixture was extracted with EtOAc (3 x 5 mL). The combined organic mixtures were washed with 5% aq LiCl (5 x 5 mL). The organic mixture was dried with Na₂SO₄, filtered, and concentrated by rotary evaporation to afford a light brown residue. The residue was purified by flash column chromatography (gradient 100% CH₂Cl₂ to 5% MeOH:CH₂Cl₂) to afford a white solid (52 mg, 99%) in 42% yield: m.p. = 246–248 °C; ¹H NMR (DMSO-d₆, 400 MHz) δ 9.90 (s, 1H), 8.90 (d, *J* = 8.4 Hz, 1H), 8.43 (d, *J* = 0.9 Hz, 1H), 7.89 (dt, *J* = 7.9, 1.0 Hz, 1H), 7.80 – 7.70 (m, 2H), 7.70

– 7.63 (m, 2H), 7.63 – 7.52 (m, 2H), 7.36 (ddd, $J = 7.9, 7.0, 1.0$ Hz, 2H); $^{13}\text{C}\{^1\text{H}\}$ NMR (DMSO- d_6 , 101 MHz) δ 167.8, 165.1, 163.7, 140.2, 139.6, 139.1, 137.5, 128.5, 126.5, 123.6, 122.8, 121.6, 116.9, 86.0; IR (film) ν 3491, 3305, 1547, 1465, 1424, 746; HRMS (ESI-TOF) m/z : $[\text{M}+\text{H}]^+$ Calcd for $\text{C}_{16}\text{H}_{13}\text{N}_7$ 430.0277; Found 430.0271.

Methyl 4-amino-6-((4-chlorophenyl)amino)-1,3,5-triazine-2-carboxylate (34): Following the general free base procedure C, a mixture of 1-carbamimidamido-N-(4-chlorophenyl)methanimidamide hydrochlorideⁱⁱ (8.9 g, 35.8 mmol) and NaOEt (2.4 mg, 35.8 mmol) was stirred in MeOH (70 mL) at rt for 22 h. Following the general procedure D, a mixture of dimethyloxalate (8.5 g, 71.6 mmol) and the arylbiguanide base (7.6 g, 35.8 mmol) in anhydrous MeOH (0.25 M) was stirred at 35 °C for 1.5 h and then refluxed overnight. The mixture was cooled to rt and the crude product was collected by filtration and washed with cold MeOH. The crude solid was triturated with MeOH to afford a white solid (7.3 g, 94% pure) in 73% yield: m.p. = 256–249 °C; ^1H NMR (DMSO- d_6 , 400 MHz) δ 10.17 (br, 1H), 7.84 (d, $J = 8.5$ Hz, 2H), 7.70 (br, 1H), 7.56 (br, 1H), 7.34 (d, $J = 8.9$ Hz, 2H), 3.84 (s, 3H); $^{13}\text{C}\{^1\text{H}\}$ NMR (DMSO- d_6 , 101 MHz) δ 167.1, 164.3, 163.9, 163.8, 138.5, 128.4, 126.1, 121.2, 52.5; IR (film) ν 3476, 3145, 1748, 1528, 1245; HRMS (ESI-TOF) m/z : $[\text{M}+\text{H}]^+$ Calcd for $\text{C}_{11}\text{H}_{11}\text{ClN}_5\text{O}_2$ 280.0596; Found 280.0608.

Methyl 4-amino-6-((4-bromophenyl)amino)-1,3,5-triazine-2-carboxylate (35): Following the general free base procedure C, a mixture of N-(4-bromophenyl)-1-carbamimidamidomethanimidamide hydrochlorideⁱ (12.4 g, 42.5 mmol) and NaOEt (2.9 g, 42.5 mmol) was stirred in EtOH (70 mL) at rt for 22 h. Following the general procedure D, a mixture of dimethyloxalate (9.1 g, 76.9 mmol) and the arylbiguanide base (9.9 g, 38.5 mmol) in anhydrous MeOH (0.21 M) was stirred at 35 °C for 1 h and then refluxed overnight for ~2.5 d. After 28 h at -20 °C, the precipitate was collected by filtration and washed with cold MeOH to afford a white solid (8.6 g) in 69% (crude). The solid was recrystallized using MeOH to afford title compound as a white solid (218 mg, 99% pure) in 18% yield: m.p. = 224–226 °C; ^1H NMR (DMSO- d_6 , 400 MHz) δ 10.17 (br, 1H, NH), 7.79 (d, $J = 8.5$ Hz, 2H), 7.70 (s, 1H), 7.60 (br s, 1H), 7.46 (d, $J = 8.9$ Hz, 2H), 3.83 (s, 3H); $^{13}\text{C}\{^1\text{H}\}$ NMR (DMSO- d_6 , 101 MHz) δ 167.1, 164.3, 163.9, 163.8, 138.9, 131.3, 121.8, 114.1, 52.5; IR (film) ν 3473, 3145, 1748, 1618, 1249, 825, 519; HRMS (ESI-TOF) m/z : $[\text{M}+\text{H}]^+$ Calcd for $\text{C}_{11}\text{H}_{11}\text{BrN}_5\text{O}_2$ 324.0091; Found 324.0095.

Methyl 4-amino-6-((4-nitrophenyl)amino)-1,3,5-triazine-2-carboxylate (36): Following the general free base procedure C a mixture of 1-carbamimidamido-N-(4-nitrophenyl)methanimidamide hydrochloride (**52**) (15.8 g, 61.1 mmol) and NaOEt (4.2 g, 61.1 mmol) was stirred in EtOH (100 mL) at rt for 22 h. Following the general procedure D, a mixture of dimethyloxalate (574 mg, 2.43 mmol) and the arylbiguanide base (540 mg, 2.43 mmol) in anhydrous MeOH (0.12 M) was stirred at 35 °C for 0.5 h and then refluxed overnight for ~2.5 d. After 24 h at -20 °C, a precipitate formed. The crude product was collected by filtration and washed with cold MeOH to afford a tan powder (130 mg, 94% pure) in 18% yield. The solid was used without further purification: m.p. = > 260 °C; ^1H NMR (DMSO- d_6 , 400 MHz) δ 10.71 (br s, 1H), 8.19 (d, $J = 9.4$ Hz, 2H), 8.09 (d, $J = 9.4$ Hz, 2H), 7.91 (br s, 1H), 7.74 (br s, 1H), 3.86 (s, 3H); $^{13}\text{C}\{^1\text{H}\}$ NMR (DMSO- d_6 , 101 MHz) δ 167.6, 164.9, 164.5, 164.0, 146.6, 141.7, 125.2, 119.5, 53.1; IR (film) ν 3413, 3368, 1744, 1644, 1502, 1335; HRMS (ES-TOF) M/Z : $[\text{M}+\text{H}]^+$ Calcd for $\text{C}_{11}\text{H}_{11}\text{N}_6\text{O}_4$ 291.0837; Found 291.0842.

Methyl 4-amino-6-((4-cyanophenyl)amino)-1,3,5-triazine-2-carboxylate (37): The general procedure C was followed using 1-carbamimidamido-N-(4-cyanophenyl)methanimidamide hydrochloride (**53**) (496 mg, 2.08 mmol), NaOMe (145.9 mg, 2.70 mmol), and 6.9 mL in anhydrous MeOH. Following the general procedure D, a mixture of the corresponding arylbiguanide base, dimethyl oxalate (737 mg, 6.24 mmol) 4.0 mL MeOH was stirred at 35 °C for 0.5 h and then refluxed for 22 h. The reaction mixture was cooled to rt. The solid was precipitated and purified by flash column chromatography (5% MeOH:CH₂Cl₂) to afford a white solid (99.8 mg, 97% pure) in 18% yield: m.p. = > 260 °C; ^1H NMR (DMSO- d_6 , 400 MHz) δ 10.47 (s, 1H), 8.03 (d, $J = 8.9$ Hz, 2H), 7.82 (s,

1H), 7.75 (d, $J = 8.8$ Hz, 2H), 7.70 (s, 1H), 3.85 (s, 3H); $^{13}\text{C}\{^1\text{H}\}$ NMR (DMSO- d_6 , 101 MHz) δ 167.6, 164.9, 164.5, 164.1, 144.4, 133.4, 120.0, 119.8, 104.2, 53.1; IR (film) ν 3402, 3357, 2229, 1733, 1655, 1238, 795, 609; HRMS (ESI-TOF) m/z : $[\text{M}+\text{H}]^+$ Calcd for $\text{C}_{12}\text{H}_{11}\text{N}_6\text{O}_2$ 271.0944; Found 271.0944.

Methyl 4-amino-6-((4-((trimethylsilyl)ethynyl)phenyl)amino)-1,3,5-triazine-2-carboxylate (38): Methyl 4-amino-6-((4-iodophenyl)amino)-1,3,5-triazine-2-carboxylate (**19**) (75 mg, 0.202 mmol), $\text{PdCl}_2(\text{PPh}_3)_2$ (76 mg, 0.108 mmol), and CuI (10 mg, 0.054 mmol) were weighed into a microwave vial with a stir bar. The flask was sealed and placed under vacuum then backfilled with N_2 . Then, trimethylsilyl acetylene (0.157 mL, 0.592 mmol), Et_3N (0.524 mL, 3.77 mmol), and THF (1.8 mL) were added, and the mixture was stirred at rt overnight. After 18 h, the mixture was diluted with EtOAc (1.0 mL) and washed with brine (3 mL x 2). The organic mixture was dried with Na_2SO_4 , filtered, and concentrated by rotary evaporation to afford a brown solid. The solid was purified by column chromatography (1–5% MeOH: CH_2Cl_2) to afford a white solid (118 mg, 99% pure) in 64% yield: m.p. = 204–206 °C; ^1H NMR (DMSO- d_6 , 400 MHz) δ 10.22 (s, 1H), 7.85 (d, $J = 8.6$ Hz, 2H), 7.71 (s, 1H, NH₂), 7.40 – 7.34 (m, 2H), 3.84 (s, 3H), 0.23 (s, 6H); $^{13}\text{C}\{^1\text{H}\}$ NMR (DMSO- d_6 , 101 MHz) δ 167.7, 164.7, 164.4, 164.2, 140.7, 132.5, 119.9, 116.0, 106.2, 93.4, 53.0, 0.50; IR (film) ν 3510, 3126, 1748, 1532, 1413, 1227; HRMS (ESI-TOF) m/z : $[\text{M}+\text{H}]^+$ Calcd for $\text{C}_{16}\text{H}_{20}\text{N}_5\text{O}_2\text{Si}$ 342.1386; Found 342.1389.

Methyl 4-amino-6-((4-(cyclopropylethynyl)phenyl)amino)-1,3,5-triazine-2-carboxylate (39): Methyl 4-amino-6-((4-iodophenyl)amino)-1,3,5-triazine-2-carboxylate (**19**) (50 mg, 0.135 mmol), $\text{PdCl}_2(\text{PPh}_3)_2$ (19 mg, 0.027 mmol), and CuI (2.6 mg, 0.014 mmol) were weighed into a microwave vial with a stir bar. The flask was sealed and placed under vacuum then backfilled with N_2 . Then, ethynylcyclopropane (12.6 μL , 0.149 mmol), Et_3N (0.131 mL, 0.945 mmol), and THF (0.43 mL) were added, and the mixture was stirred at rt overnight. After 18 h, the mixture was diluted with EtOAc (1.0 mL) and washed with brine (3 mL x 2). The organic mixture was dried with Na_2SO_4 , filtered, and concentrated by rotary evaporation to afford a brown solid. The solid was purified by column chromatography (1–5% MeOH: CH_2Cl_2) to afford a white solid (15 mg, 96% pure) in 36% yield: ^1H NMR (DMSO- d_6 , 400 MHz) δ 10.11 (s, 1H), 7.79 (d, $J = 8.3$ Hz, 2H), 7.70 – 7.40 (m, 2H), 7.28 (d, $J = 8.4$ Hz, 2H), 3.84 (s, 3H), 1.52 (tt, $J = 8.3, 5.0$ Hz, 1H), 0.99 – 0.79 (m, 2H), 0.72 (dt, $J = 5.1, 3.0$ Hz, 2H); $^{13}\text{C}\{^1\text{H}\}$ NMR (DMSO- d_6 , 101 MHz) δ 167.1, 164.2, 163.9, 163.8, 139.1, 131.6, 119.5, 116.8, 92.6, 75.8, 52.4, 8.3; IR (film) ν 3298, 3130, 1748, 1510; HRMS (ESI-TOF) m/z : $[\text{M}+\text{H}]^+$ Calcd for $\text{C}_{16}\text{H}_{16}\text{N}_5\text{O}_2$ 310.1304; Found 310.1310.

Methyl 4-amino-6-((6-iodopyridin-3-yl)amino)-1,3,5-triazine-2-carboxylate (40): The general procedure C was followed using 1-Carbamimidamido-N-(6-iodopyridin-3-yl)methanimidamide hydrochloride (**54**) (787 mg, 2.31 mmol), NaOMe (374 mg, 6.93 mmol), and 4.6 mL in anhydrous MeOH. Following the general procedure D, the corresponding arylbiguanide base, dimethyl oxalate (818 mg, 6.93 mmol) and 9.0 mL MeOH were stirred at 35 °C for 3 h and then heated at reflux for 12 h. The reaction mixture was cooled to rt and concentrated to afford a grey purple solid. The solid was purified by column chromatography (1–20% MeOH: CH_2Cl_2) to afford a light purple solid (95 mg, 95% pure) in 11% yield: m.p. = 244–246 °C; ^1H NMR (DMSO- d_6 , 400 MHz) δ 10.3 (br s, 1H), 8.87 (s, 1H), 7.91 (dd, $J = 8.6, 2.9$ Hz, 1H), 7.74 (d, $J = 8.7$ Hz, 2H), 7.62 (br s, 1H), 3.84 (s, 3H); $^{13}\text{C}\{^1\text{H}\}$ NMR (DMSO- d_6 , 101 MHz) δ 167.3, 164.6, 164.2, 163.9, 143.0, 136.8, 134.1, 129.2, 109.2, 52.8; IR (film) ν 3484, 3353, 3171, 1748, 1227, 944; HRMS (ESI-TOF) m/z : $[\text{M}+\text{H}]^+$ Calcd for $\text{C}_{10}\text{H}_{10}\text{IN}_6\text{O}_2$ 372.9910; Found 372.9903.

Methyl 4-amino-6-(quinolin-6-ylamino)-1,3,5-triazine-2-carboxylate (41): The general procedure C was followed using 1-carbamimidamido-N-(quinolin-6-yl)methanimidamide hydrochloride (**55**) (250 mg, 0.944 mmol), NaOMe (153 mg, 2.83 mmol), and 2.7 mL in anhydrous MeOH. The corresponding arylbiguanide base and dimethyl oxalate (3.34 mg, 2.83 mmol) in anhydrous 3.5 mL MeOH at reflux for 22 h. The reaction mixture was cooled to rt. The precipitate was filtered, washed with MeOH, and dried under vacuum to afford a white solid (164 mg, 99% pure) in 59% yield: m.p. = 258–260 °C; ^1H NMR (DMSO- d_6 , 400 MHz) δ 10.28 (s, 1H), 8.77 (dd, $J = 4.2, 1.7$ Hz, 1H), 8.63 (s, 1H), 8.26–8.17 (m, 1H), 8.02 (dd, $J = 9.1, 2.4$ Hz, 1H), 7.94 (d, $J = 9.1$ Hz, 1H), 7.75 (br

s, 1H), 7.60 (br s, 1H), 7.50 (dd, $J = 8.3, 4.2$ Hz, 1H), 3.87 (s, 3H); $^{13}\text{C}\{^1\text{H}\}$ NMR (DMSO- d_6 , 101 MHz) δ 167.7, 164.9, 164.5, 164.3, 149.2, 144.9, 137.9, 135.7, 129.6, 128.8, 124.6, 122.2, 115.9, 53.0; IR (film) ν 2784, 1756, 1644, 1208; HRMS (ESI-TOF) m/z : $[\text{M}+\text{H}]^+$ Calcd for $\text{C}_{14}\text{H}_{13}\text{N}_6\text{O}_2$ 297.1095; Found 297.1103.

N-[2-(1-{4-amino-6-[(4-iodophenyl)amino]-1,3,5-triazin-2-yl]-1H-1,2,3-triazol-4-yl)phenyl]methanesulfonamide (42): 6-Azido- N^2 -(4-iodophenyl)-1,3,5-triazine-2,4-diamine (**72**) (37 mg, 0.104 mmol), Et_3NH (14.5 μL , 0.104 mmol) and copper iodide (5.9 mg, 0.031 mmol) were in anhydrous DMSO (0.416 mL) under N_2 . After 15 min, N -(2- N -(2-ethynylphenyl)methanesulfonamide (20.3 mg, 0.104 mmol) was added to the mixture and stirred at rt for 2 h. The reaction progress was monitored using TLC until completion. The reaction mixture was diluted with 10% NH_3 aq (1 mL), and the mixture was extracted with EtOAc (3 x 2 mL). The combined organic mixture was washed several times with H_2O and then dried with Na_2SO_4 , filtered, and concentrated by rotary evaporation to afford a brown residue. The residue was purified by flash column chromatography (5-100% EtOAc:Hexanes) to afford a white solid (5 mg, 90% pure) in 5% yield: ^1H NMR (DMSO- d_6 , 400 MHz) δ 13.01 (s, 1H), 9.58 (s, 1H), 8.04 (dq, $J = 8.4, 0.9$ Hz, 1H), 7.79 – 7.66 (m, 3H), 7.63 – 7.57 (m, 2H), 7.37 – 7.25 (m, 2H), 7.11 (s, 2H), 6.75 (d, $J = 0.8$ Hz, 1H), 3.88 (s, 3H); $^{13}\text{C}\{^1\text{H}\}$ NMR (DMSO- d_6 , 101 MHz) δ 167.5, 164.9, 164.3, 146.4, 140.4, 137.4, 135.9, 128.2, 125.1, 123.8, 122.7, 122.3, 114.5, 95.6, 85.6, 55.8; HRMS (ESI-TOF) m/z : $[\text{M}]^-$ Calcd for $\text{C}_{10}\text{H}_8\text{Cl}_2\text{N}_4$ 253.0038; Found 253.0048.

6-(4-(4-Fluorophenyl)-1H-1,2,3-triazol-1-yl)- N^2 -(4-iodophenyl)-1,3,5-triazine-2,4-diamine (43): 6-Azido- N^2 -(4-iodophenyl)-1,3,5-triazine-2,4-diamine (**72**) (50 mg, 0.141 mmol) and copper iodide (8.1 mg, 0.0423 mmol) were in anhydrous DMSO (0.214 mL) under N_2 . After 15 min, 1-ethynyl-4-fluorobenzene (49 μL , 0.423 mmol) was added to the mixture and stirred at rt for 2 h. The reaction progress was monitored using TLC until completion. The reaction mixture was diluted with 10% NH_3 aq (1 mL), and the mixture was extracted with EtOAc (3 x 2 mL). The combined organic mixture was washed several times with H_2O and then dried with Na_2SO_4 , filtered, and concentrated by rotary evaporation to afford a yellow residue. The residue was purified by flash column chromatography (50-75% EtOAc:Hexanes) to afford a white solid (21 mg, 97% pure) in 31% yield: ^1H NMR (DMSO- d_6 , 400 MHz) δ 10.22 (s, 1H), 9.06 (s, 1H), 8.07 (dd, $J = 8.5, 5.5$ Hz, 2H), 7.78 (s, 2H), 7.68 (q, $J = 8.7$ Hz, 4H), 7.41 – 7.27 (m, 2H); $^{13}\text{C}\{^1\text{H}\}$ NMR (DMSO- d_6 , 101 MHz) δ 167.9, 165.0, 163.8 (d, $^1J_{\text{CF}} = 246.6$ Hz), 161.0, 146.1, 139.6, 137.6, 128.3 (d, $^3J_{\text{CF}} = 7.9$ Hz), 126.8 (d, $^4J_{\text{CF}} = 3.0$ Hz), 122.9, 119.6, 116.4 (d, $^2J_{\text{CF}} = 21.7$ Hz), 86.7; ^{19}F NMR (DMSO- d_6 , 365 MHz) δ -113.1; IR (film) ν 3461, 3286, 1644, 1540, 1417, 1238, 1011; HRMS (ESI-TOF) m/z : $[\text{M}+\text{H}]^+$ Calcd for $\text{C}_{17}\text{H}_{13}\text{FIN}_8$ 475.0292; Found 475.0259.

Methyl 4-amino-6-((3,5-difluorophenyl)amino)-1,3,5-triazine-2-carboxylate (44): Following the general free base procedure C, a mixture of 1-carbamimidamido- N -(3,5-difluorophenyl)methanimidamide hydrochloride¹ (152 mg, 0.607 mmol) and NaOEt (41 mg, 0.607 mmol) was stirred in EtOH (5 mL) at rt for 24 h. Following the general procedure D, a mixture of dimethyloxalate (143 mg, 1.21 mmol) and the arylbiguanide base (129 mg, 0.607 mmol) in anhydrous MeOH (0.11 M) was stirred at 25 $^\circ\text{C}$ for 0.5 h and then refluxed for 44 h. After 20 h at -20 $^\circ\text{C}$, the precipitate was collected by filtration. The solid was recrystallized using MeOH to afford a white solid (15 mg, 98% pure) in 8% yield: ^1H NMR (DMSO- d_6 , 400 MHz) δ 10.39 (s, 1H), 7.81 (s, 1H), 7.73 (s, 1H), 7.67 – 7.44 (m, 2H), 6.83 (tt, $J = 9.3, 2.4$ Hz, 1H), 3.84 (s, 3H); $^{13}\text{C}\{^1\text{H}\}$ NMR (DMSO- d_6 , 101 MHz) δ 167.6, 164.8, 164.3, 164.1, 162.9 (dd, $^1J_{\text{CF}} = 242.8$

Hz), 142.6 (t, $^3J_{CF} = 14.3$ Hz), 102.8 (d, $^2J_{CF} = 29.8$ Hz), 97.7 (t, $^2J_{CF} = 26.6$ Hz), 53.1; ^{19}F NMR (DMSO- d_6 , 365 MHz) δ -109.6; IR (film) ν 3491, 3294, 1756, 1555, 1242, 1037; HRMS (ESI-TOF) m/z : $[\text{M}+\text{H}]^+$ Calcd for $\text{C}_{11}\text{H}_{10}\text{F}_2\text{N}_5\text{O}_2$ 282.0798; Found 282.0801.

Methyl 4-amino-6-((3,5-bis(trifluoromethyl)phenyl)amino)-1,3,5-triazine-2-carboxylate (45): Following the general free base procedure C, a mixture of *N*-[3,5-bis(trifluoromethyl)phenyl]-1-carbamimidamidomethanimidamide hydrochloride (**56**) (5.6 g, 16.1 mmol) and NaOEt (1.1 g, 16.1 mmol) was stirred in EtOH (30 mL) at rt for 22 h. Following the general procedure D, a mixture of dimethyloxalate (3.8 g, 32.2 mmol) and the arylbiguanide base (5.1 g, 16.1 mmol) in anhydrous MeOH (0.21 M) was stirred at 25 °C for 2 h and then refluxed overnight for 21 h. After 48 h at -20 °C, the precipitate was collected by filtration. The solid was recrystallized from MeOH to afford a white solid (2.9 g, 99% pure) in 47% yield: ^1H NMR (DMSO- d_6 , 400 MHz) δ 10.62 (s, 1H), 8.51 (s, 2H), 7.88 (s, 1H), 7.74 – 7.63 (m, 2H), 3.85 (s, 3H); $^{13}\text{C}\{^1\text{H}\}$ NMR (DMSO- d_6 , 101 MHz) δ 167.1, 164.6, 163.9, 163.5, 141.6, 130.7 (q, $^3J_{CF} = 32.7$ Hz), 123.4 (q, $^1J_{CF} = 272.7$ Hz), 114.8 (m), 52.7; IR (film) ν 3286, 3156, 1733, 1543, 1278; HRMS (ESI-TOF) m/z : $[\text{M}+\text{H}]^+$ Calcd for $\text{C}_{13}\text{H}_{10}\text{F}_6\text{N}_5\text{O}_2$ 382.0734; Found 382.0738.

Methyl 4-amino-6-((3,5-dimethylphenyl)amino)-1,3,5-triazine-2-carboxylate (46): Following the general free base procedure C, a mixture of 1-carbamimidamido-*N*-(3,5-dimethylphenyl)methanimidamide hydrochloride (**57**) (226 mg, 0.933 mmol) and NaOEt (64 mg, 0.933 mmol) was stirred in EtOH (5 mL) at rt for 22 h. Following the general procedure D, a mixture of dimethyloxalate (3.8 g, 32.2 mmol) and the arylbiguanide base (5.1 g, 16.1 mmol) in anhydrous MeOH (0.21 M) was stirred at 25 °C for 1 h and then refluxed for 24 h. The precipitate was collected by filtration and recrystallized using MeOH to afford a white solid (53 mg, 99% pure) in 21% yield: m.p. = 214–215 °C; ^1H NMR (DMSO- d_6 , 400 MHz) δ 9.87 (br, 1 H), 7.60 (br, 1 H), 7.41 (s, 2 H), 6.66 (s, 1 H), 3.83 (s, 3 H), 2.25 (s, 6 H); $^{13}\text{C}\{^1\text{H}\}$ NMR (DMSO- d_6 , 101 MHz) δ 167.1, 164.7, 164.3, 164.0, 139.2, 137.4, 124.2, 117.9, 52.5, 21.2; IR (film) ν 3346, 3193, 1748, 1547, 1242, 795, 605; HRMS (ESI-TOF) m/z : $[\text{M}+\text{H}]^+$ Calcd for $\text{C}_{13}\text{H}_{16}\text{N}_5\text{O}_2$ 274.1299; Found 274.1308.

Methyl 4-amino-6-((3-fluoro-4-iodophenyl)amino)-1,3,5-triazine-2-carboxylate (47): The general procedure C was followed using 1-carbamimidamido-*N*-(3-fluoro-4-iodophenyl)methanimidamide hydrochloride (**60**) (200 mg, 0.559 mmol), NaOMe (118 mg, 2.18 mmol), and 1.6 mL in anhydrous MeOH. The corresponding arylbiguanide base, dimethyl oxalate (198 mg, 1.68 mmol) 1.8 mL MeOH at reflux 18 h. The reaction mixture was cooled to rt. The solid was precipitated and purified by washing several times with H_2O to afford a white solid (72 mg, 97% pure) in 33% yield: ^1H NMR (DMSO- d_6 , 400 MHz) δ 10.29 (s, 1H), 8.07 – 7.99 (m, 1H), 7.74 (s, 1H), 7.70 (dd, $J = 8.7, 7.6$ Hz, 2H), 7.64 (s, 1H), 7.33 (dd, $J = 8.6, 2.4$ Hz, 1H), 3.84 (s, 6H); $^{13}\text{C}\{^1\text{H}\}$ NMR (DMSO- d_6 , 101 MHz) δ 167.0, 164.2, 163.8, 163.6, 160.1 ($^4J_{CF} = 239.6$ Hz), 142.1 (d, $^3J_{CF} = 10.7$ Hz), 138.9 (d, $^4J_{CF} = 3.3$ Hz), 117.9, 107.3 (d, $^2J_{CF} = 29.6$ Hz), 72.8 (d, $^2J_{CF} = 26.2$ Hz), 53.0 ^{19}F NMR (DMSO- d_6 , 365 MHz) δ -94.60; IR (film) ν 3335, 3197, 1748, 1540, 1223, 791; HRMS (ESI-TOF) m/z : $[\text{M}+\text{H}]^+$ Calcd for $\text{C}_{11}\text{H}_{10}\text{FIN}_5\text{O}_2$ 389.9863; Found 389.9872.

Characterization data for arylbiguanide salts and key intermediates

1-Carbamimidamido-*N*-(4-iodophenyl)methanimidamide hydrochloride (48): The general procedure B was followed using 4-iodoaniline (18.8 g, 86 mmol) and dicyandiamide (7.2 g, 86 mmol) in 28.6 mL 3 M HCl at 90 °C for 48 h. The precipitate was then filtered to afford a grey purple solid. The solid was triturated with Et_2O and then rinsed several times with H_2O (5 x 5 mL) to afford a grey purple solid (23.2 g) in 79%: ^1H NMR (DMSO- d_6 , 400 MHz) δ 9.93 (d, $J = 3.1$ Hz, 1H), 7.62 (d, $J = 8.7$ Hz, 2H), 7.40 (s, 3H), 7.23 (d, $J = 8.8$ Hz, 2H), 7.10 (s, 2H); $^{13}\text{C}\{^1\text{H}\}$ NMR (DMSO- d_6 , 101 MHz) δ 161.3, 154.7, 138.7, 137.2, 122.7, 86.7; HRMS (ESI-TOF) m/z : $[\text{M}+\text{Na}]^+$ Calcd for $\text{C}_8\text{H}_{11}\text{ClIN}_5\text{Na}$ 361.9645; Found 361.9635.

1-Carbamimidamido-N-(3-iodophenyl)methanimidamide hydrochloride (49): The general procedure B was followed using 3-iodoaniline (500 mg, 2.28 mmol) and dicyandiamide (192 mg, 2.28 mmol) in 0.76 mL 3 M HCl at 100 °C for 24 h. The reaction mixture was concentrated by rotary evaporation and triturated with Et₂O to afford a grey purple solid (606 mg) in 78% yield: ¹H NMR (DMSO-d₆, 400 MHz) δ 10.00 (s, 1H), 7.83 (s, 1H), 7.44 (s, 3H), 7.38 (d, J = 7.9 Hz, 2H), 7.10 (dd, J = 14.7, 6.7 Hz, 3H); ¹³C{¹H} NMR (DMSO-d₆, 101 MHz) δ 161.4, 154.7, 140.4, 131.5, 130.6, 128.5, 119.7, 94.4; HRMS (ESI-TOF) m/z: [M]⁺ Calcd for C₈H₁₁IN₅ 304.0059; Found 304.0066.

1-Carbamimidamido-N-(2-iodophenyl)methanimidamide hydrochloride (50): The general procedure B was followed using 2-iodoaniline (1.0 g, 4.57 mmol) and dicyandiamide (384 mg, 4.57 mmol) in 1.5 mL 3 M HCl at 100 °C for 48 h. The reaction mixture was concentrated by rotary evaporation and triturated with Et₂O to afford a grey purple solid (953 mg) in 56% yield: ¹H NMR (DMSO-d₆, 400 MHz) δ 7.75 (s, 1H), 7.47 (d, J = 1.6 Hz, 1H), 6.66 (d, J = 8.4 Hz, 1H), 6.52 – 6.37 (m, 1H), 4.63 (s, 3H); ¹³C{¹H} NMR (DMSO-d₆, 101 MHz) δ 161.8, 156.6, 139.2, 128.9, 128.1, 127.7, 121.2, 96.5; HRMS (ESI-TOF) m/z: [M]⁺ Calcd for C₈H₁₁IN₅ 304.0059; Found 304.0058.

1-Carbamimidamido-N-(4-hydroxyphenyl)methanimidamide hydrochloride (51):³⁶ Into a microwave vessel was added 4-aminophenol (649 mg, 5.95 mmol), dicyandiamide (500 mg, 5.95 mmol), and (0.83 mL, 6.55 mmol). Then acetonitrile (7.9 mL) was added and the mixture was stirred at 150 °C. After 4.5 hours, a purple precipitate formed. The precipitate was dissolved in MeOH and stirred for 15 min, then concentrated by rotary evaporation to afford a purple solid. The solid was purified by trituration with Et₂O and provided the title compound (1.38 mg) in quantitative yield as a purple solid: ¹H NMR (DMSO-d₆, 400 MHz) δ 9.39 (s, 1H), 9.23 (d, J = 2.6 Hz, 1H), 7.09 (d, J = 8.8 Hz, 2H), 7.08-7.07 (m, 3H), 6.95 (s, 2H), 6.72 (d, J = 8.8 Hz, 2H); ¹³C{¹H} NMR (DMSO-d₆, 101 MHz) δ 161.0, 156.8, 154.8, 129.7, 124.6, 115.7; HRMS (ESI-TOF) m/z: [M]⁺ Calcd for C₈H₁₂N₅O 194.1042; Found 194.1048.

1-Carbamimidamido-N-(4-nitrophenyl)methanimidamide hydrochloride (52): The general procedure B was followed using 4-nitroaniline (15.4 g, 111.8 mmol) and dicyandiamide (9.40 g, 111.8 mmol) in 37.2 mL 3 M HCl at 90 °C for 4 d and 16 h. The reaction mixture was cooled for 6 h. The precipitate was then filtered and triturated with Et₂O (3 x) to afford an orange brown solid (15.7 mg) in 55% yield: ¹H NMR (DMSO-d₆, 400 MHz) δ 10.51 (s, 1H), 8.19 (d, J = 9.3 Hz, 2H), 7.66 (d, 9.3 Hz, 2H), 7.67-7.66 (br overlapping, 3H), 7.25 (br, 2H); ¹³C{¹H} NMR (DMSO-d₆, 101 MHz) δ 161.8, 153.6, 141.5, 124.8, 119.1, 117.5; HRMS (ESI-TOF) m/z: [M]⁺ Calcd for C₈H₁₁N₆O₂ 223.1304; Found 223.0943.

1-Carbamimidamido-N-(4-cyanophenyl)methanimidamide hydrochloride (53):³⁷ The general procedure B was followed using 4-aminobenzonitrile (1.0 g, 8.47 mmol) and dicyandiamide (712 mg, 8.47 mmol) in 2.8 mL 3 M HCl and 10 mL MeCN at 100 °C for 2 d. The precipitate was filtered and used without further purification to afford a grey solid (1.2 g) in 60% yield: ¹H NMR (DMSO-d₆, 400 MHz) δ 10.22 (s, 1H), 7.80 – 7.69 (d, J = 8.9 Hz, 2H), 7.60 (d, J = 8.5 Hz, 2H), 7.18 (broad s, 2H); ¹³C{¹H} NMR (DMSO-d₆, 101 MHz) δ 162.2, 154.3, 144.1, 133.5, 120.2, 119.7, 104.6; HRMS (ESI-TOF) m/z: [M]⁺ Calcd for C₈H₁₁N₆O₂ 223.0943; Found 223.0948.

N⁻-(Azaniumylmethanimidoyl)-N-(6-iodopyridin-3-yl)guanidine chloride (54): The general procedure B was followed using 5-amino-2-iodopyridine (500 mg, 2.27 mmol) and dicyandiamide (191 mg, 2.27 mmol) in 0.91 mL 3 M HCl and 0.91 mL H₂O at 100 °C for 24 h. The reaction mixture was concentrated by rotary evaporation and triturated with Et₂O to afford a brown solid (787 mg) in 98%: ¹H NMR (DMSO-d₆, 400 MHz) δ 8.42 (s br, 1H), 7.76–7.73 (m, 1H), 7.59–7.49 (m, 1H), 7.23–7.17 (m, 5H); ¹³C{¹H} NMR (DMSO-d₆, 101 MHz) δ 161.6, 154.4, 143.1, 136.1, 134.1, 130.0; HRMS (ESI-TOF) m/z: [MH]⁺ Calcd for C₇H₁₀IN₆ 305.0012; Found 305.0007.

1-Carbamimidamido-N-(quinolin-6-yl)methanimidamide hydrochloride (55): The general procedure B was followed using quinolin-6-amine (1.0g, 6.94 mmol) and dicyandiamide (584 mg, 6.95 mmol) in 2.31 mL 3 M HCl at 100 °C for 36 h. The precipitate was filtered, washed with H₂O, and purified by

trituration (MeOH) provided 50 (802 mg) in 44% yield as a brown solid: ^1H NMR (DMSO- d_6 , 400 MHz) δ 10.05 (s, 1H), 8.81 (dd, $J = 4.6, 2.2$ Hz, 1H), 8.30 (d, $J = 8.4$ Hz, 1H), 8.03 – 7.94 (m, 2H), 7.78 (dd, $J = 9.0, 2.4$ Hz, 1H), 7.55 – 7.48 (m, 1H), 7.44 (s, 2H), 7.17 (s, 2H); $^{13}\text{C}\{^1\text{H}\}$ NMR (DMSO- d_6 , 101 MHz) δ 161.5, 154.9, 148.6, 144.0, 137.0, 135.7, 128.9, 128.3, 124.8, 121.8, 116.0; HRMS (ESI-TOF) m/z : $[\text{M}^+]$ Calcd for $\text{C}_{11}\text{H}_{13}\text{N}_6$ 229.1202; Found 229.1207.

N-[3,5-Bis(trifluoromethyl)phenyl]-1-carbamimidamidomethanimidamide hydrochloride (56): The general procedure B was followed using 3,5-bis(trifluoromethyl)aniline (5 mL, 32.0 mmol) and dicyandiamide (2.69 g, 36.1 mmol) in 10.7 mL 3 M HCl at 90 °C for 21 h. The reaction mixture was cooled for 2.5 h. The precipitate was then filtered and triturated with Et_2O to afford a white powder (5.6 g) in 74%: ^1H NMR (DMSO- d_6 , 400 MHz) δ 10.40 (s, 1H), 8.07 (s, 1H), 7.72 (d, $J = 1.9$ Hz, 1H), 7.61 (s, 2H), 7.23 (s, 1H); $^{13}\text{C}\{^1\text{H}\}$ NMR (DMSO- d_6 , 101 MHz) δ 161.9, 154.0, 141.5, 130.6 (q, $^2J_{\text{CF}} = 32.6$ Hz), 123.2 (q, $^1J_{\text{CF}} = 272.6$ Hz), 119.8 (d, $^3J_{\text{CF}} = 4.4$ Hz), 115.2 (t, $^4J_{\text{CF}} = 3.8$ Hz); HRMS (ESI-TOF) m/z : $[\text{M}+\text{H}]^+$ Calcd for $\text{C}_{10}\text{H}_{10}\text{F}_6\text{N}_5$ 314.0840; Found 314.0840.

1-Carbamidamido-N-(3,5-dimethylphenyl)methanimidamide hydrochloride (57): The general procedure B was followed using 3,5-dimethylaniline (0.187 mL, 1.5 mmol) and dicyandiamide (126 mg, 1.5 mmol) in 0.5 mL 3 M HCl at 90 °C for 48 h. The precipitate was then filtered to afford a tan solid (284 mg) in 78%: ^1H NMR (DMSO- d_6 , 400 MHz) δ 9.75 (s, 1H), 7.31 (s, 3H), 7.10 (s, 1H), 6.99 (s, 2H), 6.69 (s, 1H), 2.22 (s, 6H); $^{13}\text{C}\{^1\text{H}\}$ NMR (DMSO- d_6 , 101 MHz) δ 161.0, 155.4, 138.5, 137.6, 124.9, 118.5, 21.0; HRMS (ESI-TOF) m/z : $[\text{M}]^+$ Calcd for $\text{C}_{10}\text{H}_{16}\text{N}_5$ 206.1406; Found 206.1402.

1-Carbamidamido-N-(3,4,5-trifluorophenyl)methanimidamide hydrochloride (58): The general procedure B was followed using 3,4,5-trifluoroaniline (875 mg, 5.95 mmol) and dicyandiamide (500 mg, 5.95 mmol) in 1.98 mL 3 M HCl and 6.0 mL acetonitrile at 150 °C for 14 h. The precipitate was filtered, washed with H_2O and purified by trituration with Et_2O provided the title compound (1.06 mg, 93% pure) in 67% yield as a light brown solid: ^1H NMR (DMSO- d_6 , 400 MHz) δ 7.36–7.32 (m, 2H), 7.11–7.07 (m, 5H) 6.34–6.30 (s, 1H); $^{13}\text{C}\{^1\text{H}\}$ NMR (DMSO- d_6 , 101 MHz) 158.1, 156.1, 154.1, 110.6 (d, $^2J_{\text{CF}} = 23.1$ Hz), 104.5 (d, $^2J_{\text{CF}} = 24.0$ Hz); HRMS (ESI-TOF) m/z : $[\text{M}]^+$ Calcd for $\text{C}_8\text{H}_9\text{F}_3\text{N}_5$ 232.0810; Found 232.0818.

1-Carbamidamido-N-(3,5-difluoro-4-iodophenyl)methanimidamide hydrochloride (59): The general procedure B was followed using 3,5-difluoro-4-iodoaniline (148 mg, 0.581 mmol) and dicyandiamide (132 mg, 0.581 mmol) in 0.193 mL 3 M HCl and 0.193 mL H_2O at 100 °C for 48 h. The reaction mixture was concentrated by rotary evaporation and triturated with Et_2O to afford a brown solid (91.8 mg) in 42%: ^1H NMR (DMSO- d_6 , 400 MHz) δ 10.29 (s, 1H), 7.66 (d, $J = 10.1$ Hz, 1H), 7.05 (s, 1H), 6.97 (s, 1H); $^{13}\text{C}\{^1\text{H}\}$ NMR (DMSO- d_6 , 101 MHz) δ 166.2, 161.8 (d, $^4J_{\text{CF}} = 239.8$ Hz), 162.8 (d, $^4J_{\text{CF}} = 238.9$ Hz), 158.5, 143.0 (d, $^2J_{\text{CF}} = 13.9$ Hz), 102.6 (d, $^2J_{\text{CF}} = 30.3$ Hz); HRMS (ESI-TOF) m/z : $[\text{M}]^+$ Calcd for $\text{C}_8\text{H}_9\text{F}_2\text{IN}_5$ 339.9871; Found 339.9876.

1-Carbamidamido-N-(3-fluoro-4-iodophenyl)methanimidamide hydrochloride (60): The general procedure B was followed using 3-fluoro-4-iodoaniline (500 mg, 2.11 mmol) and dicyandiamide (177 mg, 2.11 mmol) in 0.7 mL 3 M HCl and 1.0 mL acetonitrile at 100 °C for 18 h. The precipitate was filtered, washed with H_2O and purified by trituration with Et_2O provided the title compound (406 mg) in 54% yield as a grey purple solid: ^1H NMR (DMSO- d_6 , 400 MHz) δ 10.29 (s, 1H), 7.71 (dd, $J = 8.6, 7.5$ Hz, 1H), 7.50 (d, $J = 2.4$ Hz, 4H), 7.15 (s, 2H), 6.98 (dd, $J = 8.7, 2.3$ Hz, 1H); $^{13}\text{C}\{^1\text{H}\}$ NMR (DMSO- d_6 , 101 MHz) δ 160.9 (d, $^1J_{\text{CF}} = 240$ Hz), 161.5, 154.3, 141.2 (d, $^3J_{\text{CF}} = 10.3$ Hz), 138.6 (d, $^4J_{\text{CF}} = 3.4$ Hz), 117.8 (d, $^4J_{\text{CF}} = 2.9$ Hz), 107.2 (d, $^2J_{\text{CF}} = 29$ Hz), 73.0 (d, $^2J_{\text{CF}} = 26.2$ Hz); HRMS (ESI-TOF) m/z : $[\text{M}+\text{Li}]^+$ Calcd for $\text{C}_8\text{H}_9\text{ClIFN}_5\text{Li}$ 363.9814; Found 363.3083.

N¹-(zaniumylmethanimidoyl)-N-(4-fluorophenyl)-N-methylguanidine chloride (61): The general procedure B was followed using 4-fluoromethylaniline (0.5 mL, 4.4 mmol) and dicyandiamide (370 mg, 4.4 mmol) in 1.5 mL 3 M HCl at 90 °C for 24 h. The reaction mixture was cooled for 1 h at rt. The precipitate was filtered and triturated with Et_2O to afford a dark brown solid in 98% yield (992 mg): ^1H NMR (DMSO- d_6 , 400 MHz) δ 7.43 – 7.34 (m, 2H), 7.31 (d, $J = 13.4$ Hz, 2H), 7.23 (dd, $J = 9.9, 7.7$ Hz, 2H), 7.06 (s, 4H, s), 3.26 (s, 3H); $^{13}\text{C}\{^1\text{H}\}$ NMR (DMSO- d_6 , 101 MHz) δ 163.5, 161.0 (d, $^1J_{\text{CF}} =$

244.6 Hz), 160.2, 159.1, 158.9, 140.3 (d, $^4J_{CF} = 2.9$ Hz), 129.3 (d, $^3J_{CF} = 8.8$ Hz), 116.4 (d, $^2J_{CF} = 22.7$ Hz); HRMS (ESI-TOF) m/z: $[M]^+$ Calcd for $C_9H_{13}FN_5$ 210.1155; Found 210.1156.

4,6-Dichloro-N-(4-fluorophenyl)-1,3,5-triazin-2-amine (62):³⁹ To a solution of cyanuric chloride (3.86 mmol) in CH_2Cl_2 at 0 °C were added Na_2CO_3 (3.86 mmol) and 4-fluoroaniline (3.86 mmol). The mixture was stirred at 0 °C for 2 h and then overnight at rt. The solvent was removed by rotary evaporation and 14 mL of ice cold water was added to the residue. The precipitate was then filtered, washed with water (3 X 7 mL), and dried under vacuum to afford a white solid (865 mg) in 87% yield. The solid was used without further purification: 1H NMR (DMSO- d_6 , 400 MHz) δ 11.19 (d, $J = 2.0$ Hz, 1H), 7.67 – 7.55 (m, 2H), 7.33 – 7.22 (m, 2H); IR (film) ν 3391, 3078, 1506, 1212; HRMS (ESI-TOF) m/z: $[M+H]^+$ Calcd for $C_9H_6Cl_2FN_4$ 258.9949; Found 258.9946.

6-Chloro-N²-(4-fluorophenyl)-N⁴,N⁴-dimethyl-1,3,5-triazine-2,4-diamine (63):¹⁸ To a solution of 4,6-dichloro-N-(4-fluorophenyl)-1,3,5-triazin-2-amine (62) (300 mg, 1.16 mmol) in acetone was added K_2CO_3 (160 mg, 1.16 mmol) and dimethylamine (0.58 mL, 1.16 mmol). The mixture was stirred at 40 °C for 6 h. The solvent was removed by rotary evaporation and ice water (11 mL) was added. The residue was filtered and washed with water (3 X 11 mL). The residue was chromatographed to afford 58 (146 mg) in 47% yield as white solid: 1H NMR ($CDCl_3$, 400 MHz) δ 7.56 – 7.45 (m, 2H), 7.12 (s, 1 H), 7.07 – 6.94 (m, 2 H), 3.18 (d, $J = 12.3$ Hz, 6H); $^{13}C\{^1H\}$ NMR ($CDCl_3$, 101 MHz) δ 169.3, 165.4, 163.8, 159.4 (d, $^1J_{CF} = 244.3$ Hz), 134.2 (d, $^4J_{CF} = 2.9$ Hz), 122.3 (d, $^3J_{CF} = 7.9$ Hz), 115.8 (d, $^2J_{CF} = 22.6$ Hz), 36.9 (dd); ^{19}F NMR ($CDCl_3$, 101 MHz) δ -120.0; IR (film) ν 3309, 2929, 1201, 832; HRMS (ESI-TOF) m/z: $[M+H]^+$ Calcd for $C_{11}H_{12}ClFN_5$ 268.0760; Found 268.0764.

4-(Dimethylamino)-6-((4-fluorophenyl)amino)-1,3,5-triazine-2-carbonitrile (64): To a solution of 6-chloro-N²-(4-fluorophenyl)-N⁴,N⁴-dimethyl-1,3,5-triazine-2,4-diamine (63) (111 mg, 0.416 mmol) in anhydrous DMSO (3.5 mL) was added KCN (29 mg, 0.458 mmol). The microwave vessel was sealed and stirred at 120 °C. After 15 minutes, the solution became a light orange color. The mixture was cooled to ambient temperature and diluted with ethyl acetate (5 mL). The organic mixture was washed several times with saturated NaCl solution. The organic mixture was separated, dried with Na_2SO_4 , filtered, and concentrated by rotary evaporation. The residue was purified by column chromatography (1% MeOH: CH_2Cl_2) to afford 59 (75 mg) in 70% yield as a white solid: 1H NMR ($CDCl_3$, 400 MHz) δ 10.2 (br s, 1H), 7.71 (m, 2H), 7.28 – 7.09 (m, 2H), 3.14 (d, $J = 2.9$ Hz, 6H); $^{13}C\{^1H\}$ NMR (DMSO- d_6 , 101 MHz) δ 163.5, 163.2, 162.2, 158.1 (d, $^4J_{CF} = 234.7$ Hz), 151.0, 134.8, 122.0, 115.2 (d, $^2J_{CF} = 22.3$ Hz), 36.2; ^{19}F NMR (DMSO- d_6 , 365 MHz) δ -119.5; HRMS (ESI-TOF) m/z: $[M+H]^+$ Calcd for $C_{12}H_{12}FN_6$ 259.1102; Found 259.1112.

4,6-Dichloro-N-(4-fluorophenyl)-1,3,5-triazin-2-amine (65): 4,6-Dichloro-N-(4-fluorophenyl)-1,3,5-triazin-2-amine (62) (1.18 mmol) and sodium cyanide (1.30 mmol) were weighed into a microwave vial, anhydrous DMSO (0.25 M) and 15-crown-5 (1.30 mmol) were added. The mixture was stirred at 100 °C. After 3 h, the mixture was cooled to rt and diluted with EtOAc (5 mL). The organic mixture was washed with aqueous 5% LiCl (5 X 5 mL). The organic mixture was dried with Na_2SO_4 , filtered, and concentrated by rotary evaporation to afford a white solid. The solid was chromatographed (20% EtOAc:Hexanes) to afford a white solid (191 mg) in 66% yield: 1H NMR (DMSO- d_6 , 400 MHz) δ 10.09 (s, 1H), 9.94 (s, 1H), 8.05 (s, 2H), 7.74 (s, 4H, s), 7.27 – 7.06 (m, 2 H), 2.82 (dd, $J = 16.7, 4.8$ Hz, 3H); $^{13}C\{^1H\}$ NMR (DMSO- d_6 , 101 MHz) δ 165.8, 163.6, 157.9 (d, $^1J_{CF} = 240.5$ Hz), 135.3, 121.8, 115.11 (dd, $^3J_{CF} = 22.2, 6.0$ Hz), 27.3 (d, $J = 10.8$ Hz); ^{19}F NMR (DMSO- d_6 , 365 MHz) δ -120.6; HRMS (ESI-TOF) m/z: $[M+H]^+$ Calcd for $C_{10}H_{10}ClFN_5$ 254.0609; Found 254.0607.

4-[(4-fluorophenyl)amino]-6-(methylamino)-1,3,5-triazine-2-carbonitrile (66) 6-Chloro-N²-(4-fluorophenyl)-1,3,5-triazine-2,4-diamine (65) (1.18 mmol, 300 mg), 15-crown-5 (0.260 mL, 1.30 mmol), and sodium cyanide (64 mg, 130 mmol) were weighed into a microwave vial. Anhydrous DMSO (0.25 M) was added and the mixture was heated at 100 °C. After 8 h, the mixture was cooled to rt and diluted with 5.0 mL EtOAc. The organic mixture was washed with 5% LiCl aqueous solution (5 mL x 5). The organic mixtures were dried with Na_2SO_4 , filtered, and concentrated by rotary evaporation to afford a white

solid. The solid was chromatographed (20% EtOAc:Hexanes) to afford a white solid (191 mg) in 66% yield: $^1\text{H NMR}$ (DMSO- d_6 , 400 MHz) δ 10.24 (s, 1H), 7.20 (d, $J = 8.8$ Hz, 2H), 7.15 (d, $J = 10.5$ Hz, 2H), 2.83 (dd, $J = 10.9, 4.7$ Hz, 3H); $^{13}\text{C}\{^1\text{H}\}$ NMR (DMSO- d_6 , 101 MHz) δ 164.8, 158.1 (d, $^1J_{\text{CF}} = 245.4$ Hz), 155.3, 151.0, 134.9, 121.9 (d, $^3J_{\text{CF}} = 9.0$ Hz), 122.0, 115.2 (d, $^2J_{\text{CF}} = 22.3$ Hz), 27.2 (d); HRMS (ESI-TOF) m/z : $[\text{M}+\text{H}]^+$ Calcd for $\text{C}_{11}\text{H}_{10}\text{FN}_6$ 245.0951; Found 245.0952.

Methyl 3-[(4-fluorophenyl)amino]-5-nitrobenzoate (67)⁴⁰: Methyl 3-bromo-5-nitrobenzoate (2.58 mmol), cesium carbonate (3.87 mmol), and 2,2'-bis(diphenylphosphino)-1,1'-binaphthyl (BINAP) (0.194 mmol) were weighed into a Schlenck flask, and the flask was purged with N_2 . Anhydrous toluene (25 mL) was then added to the flask. $\text{Pd}_2(\text{dba})_2$ was weighed into a separate microwave vial and dissolved in 1.0 mL of toluene. The resulting solution was added to the Schlenck flask and the mixture was stirred at 100 °C. The reaction progress was monitored by TLC (15% EtOAc:hexanes). After 29 h, the mixture was cooled to rt and diluted with EtOAc 1.0 mL, filtered over a pad of Celite®. The mixture was concentrated by rotary evaporation and purified by flash column chromatography (50% hexanes: CH_2Cl_2) to afford a dark yellow solid in 26% yield (194 mg, 98% pure): $^1\text{H NMR}$ (DMSO- d_6 , 400 MHz) δ 8.31–8.11 (m, 1 H), 7.87–7.80 (m, 2 H), 7.18–7.02 (m, 4 H), 5.96 (s, 1 H), 3.95 (s, 3 H); $^{13}\text{C}\{^1\text{H}\}$ NMR (DMSO- d_6 , 101 MHz) δ 165.2, 159.7 (d, $^1J_{\text{CF}} = 244.3$ Hz), 149.5, 146.4, 130.0 (d, $^4J_{\text{CF}} = 2.7$ Hz); 132.6, 123.7 (d, $^3J_{\text{CF}} = 8.1$ Hz), 121.2, 116.7 (d, $^2J_{\text{CF}} = 22.7$ Hz), 114.9, 112.5, 52.8; $^{19}\text{F NMR}$ (DMSO- d_6 , 365 MHz) δ -117.5; IR (film) ν 3414, 3350, 1711, 1506, 1219, 769 cm^{-1} HRMS (ESI-TOF) m/z : $[\text{M}+\text{H}]^+$ Calcd for $\text{C}_{14}\text{H}_{12}\text{FN}_2\text{O}_4$ 291.0776; Found 291.0781.

6-Bromo-4-nitropicolinic acid (68)⁴¹: To a solution of 2-bromo-6-methyl-4-nitro-pyridine (2.07 mmol) in concentrated H_2SO_4 , CrO_3 (8.28 mmol) was added at 0 °C. The resulting solution was stirred at rt for 4 h. The mixture was then heated to 70 °C for 30 min and then cooled to rt. Ice cold H_2O (13 mL) was added slowly to afford a dark green heterogeneous solution. The mixture was allowed to stand at -20 °C overnight. The crude product was filtered and recrystallized from H_2O and MeOH to afford a white solid in 75% yield (385 mg): $^1\text{H NMR}$ (DMSO- d_6 , 400 MHz) δ 8.63 (d, $J = 1.8$ Hz, 1H), 8.50 (d, $J = 1.9$ Hz, 1H).

Methyl 6-bromo-4-nitropicolinate (69)⁴²: 6-bromo-4-nitropicolinic acid (1.21 mmol) was dissolved in anhydrous methanol followed by the addition of concentrated H_2SO_4 (0.301 mmol). The mixture was heated at reflux overnight. The reaction was monitored using TLC (100% CH_2Cl_2). After completion, the reaction was cooled to rt and the pH was adjusted to pH = 4. The mixture was concentrated by rotary evaporation and the resulting residue was dissolved in EtOAc. The organic mixture was washed with water. The aqueous layer was extracted with EtOAc (3X), dried with Na_2SO_4 , filtered, and concentrated by rotary evaporation to afford a white solid (289 mg) in 91% yield. The solid was used without further purification: $^1\text{H NMR}$ (Methanol- d_4 , 400 MHz) δ 8.69 (d, $J = 1.8$ Hz, 1H), 8.6 (d, $J = 1.8$ Hz, 1H), 4.03 (s, 3 H); HRMS (ESI-TOF) m/z : $[\text{M}+\text{H}]^+$ Calcd for $\text{C}_{13}\text{H}_{11}\text{FN}_3\text{O}_4$ 292.0729; Found 292.0734.

Methyl 6-((4-fluorophenyl)amino)-4-nitropicolinate (70)⁴³: Methyl 6-bromo-4-nitropicolinate (65) (0.766 mmol), 4-fluoro aniline (0.919 mmol), $t\text{-BuOK}$ (1.07 mmol), were weighed into a Schlenck flask. The flask was purged with a N_2 , and anhydrous toluene (5.7 mL). A solution of $\text{Pd}_2(\text{dba})_2$ and bis[(2-diphenylphosphino)phenyl] ether (DPEPhos) in 2 mL of anhydrous toluene was added to the flask. The mixture was stirred at 100 °C, and the reaction progress was monitored by TLC (20% EtOAc:hexanes). After 48 h, the reaction was cooled to rt. The solution was washed with water, and the aqueous layer was extracted with EtOAc (3 x 5 mL). The combined organic layers were dried with Na_2SO_4 , filtered, and concentrated by rotary evaporation. The residue was purified by flash column chromatography (15% EtOAc:Hexanes) and then (100% CH_2Cl_2) to afford an orange solid in 14% yield (32 mg, 99% pure): $^1\text{H NMR}$ (CDCl_3 , 400 MHz) δ 8.14 (d, $J = 1.8$ Hz, 1H), 7.51 (d, $J = 1.8$ Hz, 1H), 7.38 – 7.28 (m, 2H), 7.19 – 7.10 (m, 2H), 7.08 (s, 1H), 4.03 (s, 3H); $^{13}\text{C}\{^1\text{H}\}$ NMR (CDCl_3 , 101 MHz) δ 164.3, 161.9, 151.1 (d, $^1J_{\text{CF}} = 274.8$ Hz), 158.6, 149.6, 134.3 (d, $^4J_{\text{CF}} = 3.1$ Hz), 125.1 (d, $^3J_{\text{CF}} = 8.3$ Hz), 117.1 (d, $^2J_{\text{CF}} = 22.9$ Hz), 108.9, 103.5, 53.6; $^{19}\text{F NMR}$ (methanol- d_4 , 365 MHz) δ -122.6; HRMS (ESI-TOF) m/z : $[\text{M}+\text{H}]^+$ Calcd for $\text{C}_{13}\text{H}_{11}\text{FN}_3\text{O}_4$ 292.0729; Found 292.0734.

4-Azido-6-chloro-N-(4-iodophenyl)-1,3,5-triazin-2-amine (71): To a solution of 2-azido-4,6-dichloro-1,3,5-triazine (505 mg, 2.64 mmol) in acetone was added K_2CO_3 (365 mg, 2.64 mmol) and 4-iodoaniline (578 mg, 2.64 mmol). The resulting mixture was stirred at rt for 6 h. The solvent was removed by rotary evaporation. The resulting residue was mixed with 11 mL of ice water. The solid was filtered and washed with H_2O several times to afford a white solid (820 mg) in 83% yield. The solid was used without further purification: 1H NMR (DMSO- d_6 , 400 MHz) δ 10.68 (br, 1H), 7.69 (d, $J = 8.9$ Hz, 2H), 7.49 (d, $J = 8.9$ Hz, 2H); $^{13}C\{^1H\}$ NMR (DMSO- d_6 , 101 MHz) δ 170.7, 169.9, 165.1, 138.3, 137.8, 123.4, 88.3 (2 unresolved carbons); HRMS (ESI-TOF) m/z : $[M+H]^+$ Calcd for $C_9H_6ClIN_7$; 373.9413; Found 373.9418.

6-Azido- N^2 -(4-iodophenyl)-1,3,5-triazine-2,4-diamine (72): Ammonium hydroxide (0.375 mL, 3.21 mmol) was added to 4-azido-6-chloro-N-(4-iodophenyl)-1,3,5-triazin-2-amine (400 mg, 1.07 mmol) in THF (2.9 mL). The reaction was refluxed overnight. The solution turned into a yellow color and a white solid precipitated. The mixture was concentrated by rotary evaporation to afford a white solid. The solid was purified by flash column chromatography (15–50% EtOAc:Hexanes) to afford a white solid (222 mg) in 59% yield: 1H NMR (DMSO- d_6 , 400 MHz) δ 9.80 (br, 1H), 7.60 (m, 4H), 7.50 (d, $J = 8.9$ Hz, 2H); $^{13}C\{^1H\}$ NMR (DMSO- d_6 , 101 MHz) δ 168.9, 167.8, 165.1, 139.9, 137.5, 122.7, 86.2; HRMS (ESI-TOF) m/z : $[M+H]^+$ Calcd for $C_9H_8IN_8$; 354.9912; Found 354.9920.

6-(Azidomethyl)- N^2 -(4-iodophenyl)-1,3,5-triazine-2,4-diamine (73)⁴⁴: A mixture of 6-(chloromethyl)- N^2 -(4-iodophenyl)-1,3,5-triazine-2,4-diamine (100 mg, 0.277 mmol) and sodium azide (54 mg, 0.830) were weighed into a microwave vial with a stir bar. Acetonitrile (2.8 mL) was added and the reaction vessel was sealed. The reaction was heated at reflux overnight. The mixture was cooled to rt and concentrated by rotary evaporation to afford a white residue, which was dissolved with 3 mL CH_2Cl_2 . The organic mixture was washed with H_2O , dried with Na_2SO_4 , filtered, and concentrated by rotary evaporation to afford a light grey solid. The solid was purified by column chromatography (1–5% MeOH: CH_2Cl_2) to afford a white solid (43 mg) in 42% yield: 1H NMR (DMSO- d_6 , 400 MHz) δ 9.80 (s, 1H), 9.72 (s, 1H), 7.65 (d, $J = 6.6$ Hz, 2H), 7.58 (d, $J = 8.9$ Hz, 2H), 7.29 (s, 2H), 4.18 (s, 2H); $^{13}C\{^1H\}$ NMR (DMSO- d_6 , 101 MHz) δ 173.5, 167.1, 164.5, 140.1, 137.5, 122.7, 85.9, 54.2; HRMS (ESI-TOF) m/z : $[M+H]^+$ Calcd for $C_{10}H_{10}IN_8$; 369.0073; Found 369.0066.

ASSOCIATED CONTENT

SUPPORTING INFORMATION

The Supporting Information is available free of charge on the ACS Publications website

Complete set of supplementary Figures S1–S9, Tables S1–S5, detailed procedures for chemical synthesis. Spectral data for chemical compounds is also included (PDF).

AUTHOR CONTRIBUTIONS

¹R.P.-S. (conceptualization, writing-original draft, synthesized all SAR targets, biochemical evaluation for the Toll like receptor signaling pathways, and assisted in data interpretation of biochemical data) and ²L. S. (conceptualization, writing-original draft, biochemical evaluation of inhibitors) contributed equally. ³X. K. and ³S. Z. (docking studies) and ¹R. A. (assisted in synthesis of SAR targets).

DECLARATION OF INTERESTS

Authors have a pending patent application as a potential competing interest.

ACKNOWLEDGEMENTS

This work was funded by the National Key R&D Program of China (no. 2017YFA0505200), the National Natural Science Foundation of China (no.21572114), and the National Institute of Health (RO1 GM101279) and (RO1 GM10103843). We thank Dr. Karolin Luger for providing biological reagents and research materials for the DNA intercalation studies and Dr. Johannes Rudolph for his help with conducting the DNA intercalation experiments.

REFERENCES

1. (a) Bryant, C. E.; Orr, S.; Ferguson, B.; Symmons, M. F.; Boyle, J. P.; Monie, T. P. International union of basic clinical pharmacology. XCVI. pattern recognition receptors in health and disease *Pharmacol.* **2015**, *67*, 462–504. (b) Junt, T.; Barchet, W. Translating nucleic acid-sensing pathways into therapies *Nat. Rev. Immunol.* **2015**, *15*, 529–544. (c) He, S.; Mao, X.; Sun, H.; Shirakawa, T.; Zhang, H.; Wang, X. Potential therapeutic targets in the process of nucleic acid recognition: opportunities and challenges *Trends in Pharmacol. Sci.* **2015**, *36*, 51–64.
2. Sun, L.; Wu, J.; Du, F.; Chen, X.; Chen, Z.; Cyclic GMP-AMP synthase is a cytosolic DNA sensor that activates the type I interferon pathway *Science* **2013**, *339*, 786–791.
3. Barber, G. N. STING: infection, inflammation and cancer *Nat. Rev. Immunol.* **2015**, *15*, 760–770.
4. Barrat, F. J.; Elkon, K. B.; Fitzgerald, K. A. Importance of nucleic acid recognition in inflammation and autoimmunity *Ann. Rev. Med.* **2016**, *67*, 323–336.
5. Wu, J.; Chen, Z. Innate immune sensing and signaling of cytosolic nucleic acids *Annul Rev. Immunol.* **2014**, *32*, 461–488.
6. Crow, Y. J. Type I interferonopathies: mendelian type I interferon up-regulation *Curr. Opin. Immunol.* **2015**, *32*, 7–12.
7. Ablasser, A.; Hemmerling, I.; Schmid-Burgk, J. L.; Behrendt, R.; Roers, A.; Hornung, V. J. TREX1 deficiency triggers cell-autonomous immunity in a cGAS-dependent manner *Immunol.* **2014**, *192*, 5993–5997.
8. Liu, Y. et al. Activated STING in a vascular and pulmonary syndrome *N. Engl. J. Med.* **2014**, *271*, 507–518.
9. Ng, K. W.; Marshall, E. A.; Bell, J. C.; Lam, W. L. cGAS–STING and cancer: dichotomous roles in tumor immunity and development *Trends in Immunology* **2018**, *39*, 44–54.
10. Wang, M.; Soorshjani, M. A.; Mikek, C.; Opoku-Temeng, C.; O Sintim, H. Suramin potently inhibits cGAMP synthase, cGAS, in THP-1 cells to modulate IFN- β levels *Future Med. Chem.* **2018**, *11*, 1301-1317.
11. An, J.; Woodward, J. J.; Sasaki, T.; Minie, M.; Elkon, K. B. Cutting edge: antimalarial drugs inhibits IFN- β production through blockade of cyclic GMP-AMP synthase- DNA interaction *J. Immunol.* **2015**, *194*, 4089-4093.
12. (a) Lama L.; et al. Development of human cGAS-specific small molecule inhibitors for repression of dsDNA triggered interferon expression *Nature Commun.* **2019**, *10*, 1–14. (b) Vincent J. J.; et al. Small molecule inhibition of cGAS reduces interferon expression in primary macrophages from autoimmune mice *Nature Commun.* **2017**, *8*, 1–13.
13. Dai, J. et al. Acetylation blocks cGAS activity and inhibits self-DNA-induced autoimmunity *Cell* **2019**, *176*, 1447–1460.
14. Zhang, X.; Wu, J.; Du, F.; Xu, H.; Sun, L.; Chen, Z.; Brautigam, C. A.; Zhang, X.; Chen, Z. J. The cytosolic DNA sensor cGAS forms an oligomeric complex with DNA and undergoes switch-like conformational changes in the activation loop *Cell Rep* **2014**, *6*, 421–430.

15. Hall, J. et al. Discovery of PF-06928215 as a high affinity inhibitor of cGAS enabled by a novel fluorescence polarization assay *Plos ONE* **2017**, *12*, e0184843.
16. Zhou, W.; Whiteley, A. T.; de Oliveira Mann, C. C.; Morehouse, B. R.; Nowak, R. P.; Fischer, E. S.; Gray, N. S.; Mekalanos, J. J.; Kranzusch, P. J. Structure of the Human cGAS-DNA complex reveals enhanced control of immune surveillance *Cell* **2018**, *174*, 300–311.
17. Zhang, X., Wu, J., Du, F., Xu, H., Sun, L., Chen, Z., Brautigam, C.A., Zhang, X., Chen, Z.J. The cytosolic DNA sensor cGAS forms an oligomeric complex with DNA and undergoes switch-like conformational changes in activation loop *Cell Rep.* **2014**, *6*, 421–430.
18. Kranzusch, P. J.; Lee, A. S.; Berger, J. M.; Doudna, J. Structure of human cGAS reveals a conserved family of second-messengers enzymes in innate immunity *Cell Rep.* **2013**, *3*, 1362–1368.
19. Kothayer, H.; Elshanawani, A. A.; Abu Kull, M. E.; El-Sabbagh, O. I.; Shekhar, M. P. V.; Brancale, A.; Jones, A. T.; Westwell, A. D. Design, synthesis and in vitro anticancer evaluation of 4,6-diamino-1,3,5-triazine-2-carbohydrazides and -carboamides *Bioorg. Med. Chem. Lett.* **2013**, *23*, 6886–6889.
20. (a) Wilcken, R.; Zimmermann, M. O.; Lange, A.; Joerger, A. C.; Boeckler Principles and applications of halogen bonding in medicinal chemistry and chemical biology *J. Med. Chem.* **2013**, *56*, 1363–1388. (b) Voth, A. R.; Kuu, P.; Oishi, K.; Ho, S. Halogen bonds as orthogonal molecular interactions to hydrogen bonds *Nat. Chem.* **2009**, *1*, 74–79. (c) Politzer, P. Murray, J. S.; Clark, T. Halogen bonding: an electrostatically -driven highly directional noncovalent interaction *Phys. Chem. Chem. Phys.* **2010**, *12*, 7748–7757.
21. Meanwell, N. A. Synopsis of some recent tactical application of bioisosteres in drug design *J. Med. Chem.* **2011**, *54*, 2529–2591.
22. Wilcken, R.; Zimmermann, M. O.; Bauer, M. R.; Rutherford, T. J.; Fersht, A. R.; Joerger, A. C.; Boeckler, F. M. Experimental and theoretical evaluation of the ethynyl moiety as a halogen bioisostere *ACS Chem. Biol.* **2015**, *10*, 2725–2732.
23. Huttunen, K. M.; Rauino, H.; Rautio, J. Pro-drugs from serendipity to rational design *Pharmacol. Rev.* **2011**, *63*, 750–771.
24. (a) Tanji, H.; Ohto, U.; Shibata, T.; Miyake, K.; Shimizu, T. Structural reorganization of the Toll-like receptor 8 dimer induced by agonistic ligands *Science* **2013**, *339*, 1426–1429. (b) Tanji, S.; Ohto, U.; Shibata, T.; Taoka, M.; Yamauchi, Y.; Isobe, T.; Miyake, K.; Shimizu, T. Toll-like receptor 8 senses degradation products of single-stranded RNA *Nat. Struct. Mol. Biol.* **2015**, *22*, 109–115. (c) Ohto, U.; Tanji, H.; Shimizu, T. Structure and function of toll-like receptor 8 *Microbes Infect.* **2014**, *16*, 273–282.
25. Li, X.; Shu, C.; Yi, G.; Chaton, C. T.; Shelton, C. L.; Diao, J.; Zuo, X.; Kao, C. C.; Herr, A. B.; Li, P. Cyclic GMP-AMP synthase is activated by double-stranded DNA-induced oligomerization *Immunity* **2013**, *39*, 1019–1031.
26. A. J.; Woodward, J. J.; Sasaki, T.; Minie, M.; Elkon, K. B. Cutting edge: antimalaria drugs inhibit IFN- β production through blockade of cyclic GMP-AMP synthase–DNA interaction *J. Immunol.* **2015**, *194*, 4089–4093.
27. Kothyer, H.; Morelli, M.; Brahemi, G.; Elshanawani, A. A.; Abu Kull, M. E.; El-Sabbagh, O. I.; Shekhar, M. P. V. ; Westwell, A. D. Optimised synthesis of diamino-triazinylmethylbenzoates as inhibitors of Rad6b ubiquitin conjugating enzyme *Tetrahedron Lett.* **2014**, *55*, 7015-7018.
28. LeBel, O.; Maris, T.; Duval, H.; Wuest, J. D. A practical guide to arylbiguanides synthesis and structural characterization *Can. J. Chem.* **2005**, *83*, 615-625.
29. Kim, H. W.; Lee, J. S.; Heo, H. J.; Lee, H. B.; Jeong, J. K., Park, J. H.; Kim, S.; Lee, Y. W. Biguanide compounds and use thereof, US Patent 201500126518, May 7, 2015.

- 1
2
3
4
5
6
7
8
9
10
11
12
13
14
15
16
17
18
19
20
21
22
23
24
25
26
27
28
29
30
31
32
33
34
35
36
37
38
39
40
41
42
43
44
45
46
47
48
49
50
51
52
53
54
55
56
57
58
59
60
30. Neelaput, R.; Holze, D. L.; Velaparthi, S.; Bai, H.; Brunsteinert, Blond, S. Y.; Petukhov, P. A. J. Design, synthesis, docking, and biological evaluation of novel diazide-containing isoxazole- and pyrazole-based histone deacetylase probes *Med. Chem.* **2011**, *54*, 4350–4364.
 31. (a) Sham, Y. Y.; Chu, Z. T.; Warshel, A. Consistent calculation of pK_a's of ionizable residues in proteins: semi-microscopic and microscopic approaches *J. Phys. Chem. B* **1997**, *101*, 4458–4472. (b) Repic, M.; Purg, M.; Vianello, R.; Mavri, J. Examining electrostatic preorganization in monoamine oxidases a and by structural comparison and pK_a calculations *J. Phys. Chem. B* **2014**, *118*, 4326–4332. (c) Czerwinski, R. M.; Harris, T. K.; Massiah, M. A.; Mildvan, A. S.; Whitman, C. P. The structural basis for the perturbed pK_a of the catalytic base in 4-oxalocrotonate tautomerase: kinetic and structural effects of mutations of Phe-50 *Biochemistry* **2001**, *40*, 1984–1995. (d) Stivers, J. T.; Abeygunawardana, C.; Mildvan, A. S. 4-Oxalocrotonate tautomerase: pH dependence of catalysis and pK_a values of active site residues *Biochemistry* **1996**, *35*, 814–823.
 32. Kothayer, H.; Elshahawani, A. A.; Abu Kull, M. E.; El-Sabbagh, O. I.; Shekhar, M. P. V.; Brancale, A.; Jones, A. T.; Westwell, A. D. Design, synthesis and in vitro anticancer evaluation of 4,6-diamino-1,3,5-tirazine-2-carbohydrazides and -carboxamides *Bioorg. Med. Chem. Lett.* **2013**, *23*, 6886–6889.
 33. Kim, H. w.; Jeong, J. K.; Lee, J. S.; Heo, H. J.; Lee, H. B.; Kook, J. A.; Kim, S. Q. Biguanide compound and use thereof, European Patent 3,222,614, 2017, September 8, 2017.
 34. Shima, T.; Muraoka, T.; Hoshino, N.; Akutagawa, T.; Kobayashi, Y.; Kinbara, K. Thermally driven polymorphic transition prompting a naked-eye-detectable bending and straightening motion of single crystals *Angew. Chem. Int. Ed.* **2014**, *53*, 7173–7178.
 35. Kaboudin, B.; Kazemi, F.; Pirouz, M.; Khoshkhou, A. B.; Kato, J.; Yokomatsu, T. Iron(III) chloride/L-proline as an efficient catalyst for the synthesis of 3-substituted 1,2,4-oxadiazoles from aminoximes and triethyl orthoformate *Synthesis* **2016**, *48*, 3597–3602.
 36. Obianom, O. N.; Coutinho, A. L.; Yang, W.; Yang, H.; Xue, F.; Shu, Y. Incorporation of a biguanide scaffold enhances drug uptake by organic cation transporters 1 and 2 *Mol. Pharmaceutics* **2017**, *14*, 2726 – 2739.
 37. Mayer, S.; Daigle, D. D.; Brown, E. D.; Khatri, J.; Organ, M. G. An expedient and facile one-step synthesis of a biguanide library by microwave irradiation coupled with simple product filtration. Inhibitors of dihydrofolate reductase *J. Comb. Chem.* **2004**, *6*, 776-782.
 38. Newton, A. S.; Luca, D.; Puleo, D. E.; Cisneros, J. A.; Schlessinger, J.; Jorgensen, W. W. JAK2 JH2 Fluorescence polarization assay and crystal structures for complexes with three small molecules *ACS Med. Chem. Lett.* **2017**, *8*, 614 – 617.
 39. Zheng, M.; Xu, C.; Ma, J.; Sun, Y.; Du, F.; Liu, H.; Lin, L.; Li, C.; Ding, J.; Chen, K.; Jiang, H. Synthesis and antitumor evaluation of a novel series of triaminotriazine derivatives *Bioorg. Med. Chem.* **2007**, *15*, 1815–1827.
 40. Mori, M.; Vignaroli, G.; Cau, Y.; Dinic, J.; Hill, R.; Rossi, M.; Colecchia, D.; Pesic, M.; Link, W.; Chiariello, M.; Ottmann, C.; Botta, M. Discovery of 14-3-3 protein-protein interaction inhibitors that sensitize multidrug-resistant cancer cell to doxorubicin and the Akt inhibitor GSK690693 *Chem. Med-Chem.* **2014**, *9*, 973–983.
 41. Buttelmann, B. Alanine, A.; Bourson, A.; Gill, R.; Heitz, M.; Mutel, V.; Pinard, E.; Trube, G.; Wyler, R. 2-(3,4-Dihydro-1H-isoquinolin-2-yl)-pyridines as a novel class of NR1/2B subtype selective NMDA receptor antagonists *Bioorg. Med. Chem. Lett.* **2003**, *13*, 829–832.
 42. Harmolfs, K.; Mancuso, L.; Drung, B.; Sasse, F.; Kirschning, A. Beilstein Preparation of new alkyne-modified ansamitocins by mutasynthesis *J. Org. Chem.* **2014**, *10*, 535–543.
 43. Chu, J.; Huang, H.; Hsu, W.; Chen, S.; Wu, M. Palladium(II)-catalyzed direct ortho arylation of 4-methyl-N-phenylpyridin-2-amines via C–H activation/C–C coupling and synthetic applications *Organometallics* **2014**, *33*, 1190–1204.

- 1
2
3
4
5
6
7
8
9
10
11
12
13
14
15
16
17
18
19
20
21
22
23
24
25
26
27
28
29
30
31
32
33
34
35
36
37
38
39
40
41
42
43
44
45
46
47
48
49
50
51
52
53
54
55
56
57
58
59
60
44. Ameen, M. A.; Karsten, S.; Liebscher, J. A convenient method of constructing novel tetrahydropyrido[4',3':4,5]thieno[2,3-d]-pyrimidinones-carbohy-
drate and amino acid conjugates via copper(I)-catalyzed alkyne-azide 'Click Chemistry' *Tetrahedron* **2010**, 66, 2141–2147.

"For Table of Contents Only"

